

Green Metrics in a Cyclocondensation Reaction

Supporting Information

Experiment Notes

Product Isolation.....	6
Physical Properties.....	7
Green Metrics determination.....	7
Characterization Data.....	8

Schemes

Structure of [BMIM][BF ₄].....	8
Reaction Mechanism.....	9

Figures

Photos of the Experiment.....	10
General Procedures.....	11
¹ H and ¹³ C NMR spectra.....	13
GC-MS spectra.....	14
Thermal Analysis.....	15
Schematic conclusions.....	15

- The experiment aims to prepare 1-(pentafluorophenyl)-4,5-dihydro-1*H*-pyrazoles through a cyclocondensation reaction between 1,1,1-trifluoro-4-methoxy-3-penten-2-one (enone) and pentafluorophenyl hydrazine. Two methods are presented, one under solvent free conditions with microwave irradiation (MW) and the other in ionic liquid 1-butyl-3-methylimidazolium tetrafluoroborate ([BMIM][BF₄]) (**Scheme SM 4.1.3.1.1**) under conventional thermal heating.
- All the reactants can be obtained commercially.
- The [BMIM][BF₄] and the enone can also be obtained following procedures in Frizzo et al.¹ and Martins et al.,² respectively.
- All the properties of the reactants and the final product can be seen in **Table SM 4.1.3.1.1**.

- The time needed for the class session was established in 4 h, with some time for discussion, however this part of the class can be adapted/enlarged if necessary.
- A photo and a schematic representation of experimental procedure in the conventional method are depicted in the **Figure SM 4.1.3.1.1**. The round-bottom flask in the initial and final reaction stages are depicted in **Figure SM 4.1.3.1.2**.
- In the MW method, enone (1 mmol) and hydrazine (1.2 mmol) must be mixed in a flask with a magnetic stirrer and placed in the MW apparatus (**Figure SM 4.1.3.1.3**), the mixture must be set at 100 °C for 6 min. **Figure SM 4.1.3.1.4** shows the reaction mixture in the MW flask before and after synthesis. **Figure SM 4.1.3.1.5** shows the final product after extraction.
- To evaluate the synthesis methods and support a sustainable route some aspects were considered with the aid of tools such as Atom Economy (AE), Reaction Mass Efficiency (RME) and E-factor. A comparison of these parameters in both methods is useful to demonstrate the waste production in a chemical reaction.³
- Atom Economy (AE) calculates how much of the reactant remains in the desired product regardless of the steps to obtain it.⁴ Reaction yield as well the use of solvents, auxiliaries, and molar excesses of reactants are not considered in the calculation. An ideal reaction has an AE of 100 %. For most reactions, this value can never be reached owing to the nature of the reaction. The AE was calculated according to **Eq. SM 4.1.3.1.1**.

$$AE = \left(\frac{mw_P}{mw_{R1} + mw_{R2}} \right) \times 100 \quad \text{(Eq. SM 4.1.3.1.1)}$$

Where, mw_P is the molecular weight of product P, mw_{R1} is the molecular weight of reactant R1, and mw_{R2} is the molecular weight of reactant R2.

- Reaction Mass Efficiency (RME) takes into account the mass of all reactants used, the obtained yields, and the AE. RME calculates the percentage of the mass of the reactants that remains in the product⁵, following **Eq. SM 4.1.3.1.2**.

$$\text{RME} = \left(\frac{\text{mass of P (g)}}{\text{mass of R1 (g) + mass of R2 (g)}} \right) \times 100 \quad \text{(Eq. SM 4.1.3.1.2)}$$

Where, mass of P is the mass of the isolated product, and mass of R1 and mass of R2 are the masses of reactants R1 and R2, respectively, input to obtain mass of P.

- RME values indicate lower waste generated in the synthesis reaction. The E-factor is the ratio of the generated waste weight and the total weight of the end product, a useful tool for the evaluation of rapid processes.^{6,7,8} The value is obtained following **Eq. SM 4.1.3.1.3**.

$$\text{E - factor} = \left(\frac{m_{\text{reactants}} - m_{\text{product}}}{m_{\text{product}}} \right) = \left(\frac{m_{\text{input materials}} - m_{\text{product}}}{m_{\text{product}}} \right) \quad \text{(Eq. SM 4.1.3.1.3)}$$

Where, $m_{\text{reactants}}$ is the sum of the reactant masses and m_{product} is the mass of the final product. The E-factor accounts for the actual amount of waste produced in the process and $m_{\text{input materials}}$ can be generally defined as everything but the desired product.

- The E-factor values can be obtained in different reaction steps, for the synthesis step (SYS), for the synthesis and product isolation steps (SYS + PIS), and for the synthesis and workup steps (SYS + PIS + PPS),⁹ as can be seen in **Figure SM 4.1.3.1.6**. The two first situations can be calculated for both methods. The E-factor calculation including the third step (PPS) can be applied only for the MW method, which requires the use of solvent (60 mL hexane) in a final crystallization step. Higher E-factor values obtained reflect a larger amount of waste produced in the reaction and lower E-factor values indicate lower waste generation. However, the ideal E-factor, of zero, is extremely difficult to attain.
- In this experiment, the E-factor was calculated based on the two first steps for the conventional method. For the synthesis under MW conditions, where purification is needed, the E-factor was calculated for all steps. Ionic liquid and water are not computed in the E-factor because they can be recovered after

separation of the product.⁶ A summary of the general concepts of the utilized tools can be seen in **Table SM 4.1.3.1.2**.

- The reaction can be accomplished with high product yields, in a range around 82 to 94 % in the MW method and between 74 to 83 % under conventional heating.⁹
- The ¹H and ¹³C NMR spectra of the final product are shown in **Figure SM 4.1.3.1.7** and **Figure SM 4.1.3.1.8**, respectively. The presence of two hydrogen atoms from C4 of the pyrazole ring and hydrogen atoms from the methyl group (C6) are observed. It can also be seen that H4 and H4' have a particular characteristic, which can be discussed with students. These hydrogen atoms are diastereotopic, neighbors to a chiral carbon (C5). This particularity confers to the spectrum a signal of double doublet, since each hydrogen atom presents a different coupling with the C5.
- In the ¹³C NMR it is possible to observe C-F couplings at C5 and C7. Both resulted in a quartet with different coupling constants (J). C5 is bound to the CF₃ group with a ²J = 31 Hz and C7 is bound (CF₃ group) with ¹J = 285 Hz. Furthermore, the PhF₅ (pentafluorophenyl) signals can be observed in regions around 140 ppm.
- A proposed mechanism was presented by Martins et. al (2008),¹⁰ and can be observed in **Scheme SM 4.1.3.1.2**. The reaction starts by a Michael addition to the beta-carbon atom of the enone followed by elimination of methanol after proton exchange. At first, the nitrogen (NH₂), attacks the π*-orbital from the β-carbon, dislocating the double bond. The attack mentioned above take place since the NH₂ in question is the most nucleophilic center of hydrazine. The enaminketone intermediate, in equilibrium with the imineketone form, undergoes cyclization by the addition of a second NH function to the carbonyl carbon. The nitrogen (NH), attacks the π*-orbital of the carbonyl carbon

presented in the ketone. The final step leads to formation of the product 3-Methyl-1-(pentafluorophenyl)-5-(trifluoromethyl)-4,5-dihydro-5-hydroxy-1H-pyrazole.

- **Figure SM 4.1.3.1.9** shows the CG-MS spectrum of the final product. The thermal analysis, presented in **Figure SM 4.1.3.1.10**, provides the decomposition temperature (around 151.66 °C) of the product obtained. This information indicates that there is possibility of product decomposition occurring at the temperature employed in the reaction.
- The AE and RME values obtained by Martins et. al (2013) are given in **Table SM 4.1.3.1.3**. The AE found was less than 100 % owing to the formation of methanol as a by-product. It is worth noting that product formation occurs in only one step, showing the synthesis efficiency in maintaining the reagent atoms in the final product.
- It is possible to observe that although the reaction occurs with good AE, the poor yield in the conventional thermal heating process contributed to a lower RME value when compared with the MW method.
- The E-factor results can be seen in **Table SM 4.1.3.1.4**, demonstrating that the best values were found in reactions performed in the MW method, when only the SY step is considered in the calculation. When the product extraction solvent was added to the equation, the E-factor values increased dramatically. This is a consequence of the high amount of ethyl acetate (40 mL) and drying agent (MgSO₄, 3.25 g) used in the extraction step, despite the fact that the MW reaction is solvent-free. When considering the purification step (PPS) in the MW method, the E-factor presents higher values, since 60 mL of hexane was added for product recrystallization.
- When the experiment was conducted by an organic chemistry undergraduate student, the obtained results showed the same tendency from the paper by Martins et al. (2013) (**Tables SM 4.1.3.1.3** and **SM 4.1.3.1.4**).⁹

- The student have as pre-requisite classes a basic organic chemistry and general experimental chemistry. The obtained results are presented in **Tables SM 4.1.3.1.3 and SM 4.1.3.1.4**. Since, RME and E-factor take into account the yield, was observed a difference in the values when compared with the paper.
- An essential information for the students is the importance of including solvents and drying agents when computing E-factor values. This leads to the understanding of the role of this step in the generation of waste at the laboratory scale.
- It is also important to note, in this experiment, some particularities of the E-factor values: (i) Dichloromethane and [BMIM][BF₄] are toxic as ethyl acetate, but this fact is not considered. (ii) The amount of solvent used in the extraction step (in both methods) is more important than the yield when determining the E-factor values.
- Schematic conclusions are given in **Figure SM 4.1.3.1.11**.
- AE is more useful in the comparison of two routes to obtain the same desired product, but it can also be useful as an organizing concept in combination with other metrics.
- RME and E-factor take into account the yield of the reaction and the need for a molar excess. In particular, E-factor takes into account the solvent and drying agents (and other inputs) that are not computed in RME.
- RME and E-factor appear to be a useful metric to focus on deriving chemical procedures that may lead to more sustainable practices.

Table SM 4.1.3.1.1. Physical properties for reactants and final product.

Compound	Chemical formula	Molecular mass (g mol ⁻¹)	Density (g cm ⁻³) ^a	Melting point (°C)	Boiling point (°C)
Magnesium sulfate	MgSO ₄	120.37	2.66	1124	-
Sodium sulfate	Na ₂ SO ₄	142.04	2.68	884	-
Ethyl acetate	C ₄ H ₈ O ₂	88.11	0.902	-	76.5-77.5
Dichloromethane	CH ₂ Cl ₂	84.93	1.325	-	39.8-40.0
Hexane	C ₆ H ₁₄	86.18	0.655	-	68.0
Pentafluorophenyl hydrazine	C ₆ H ₃ F ₅ N ₂	198.09	1.691	74-76	-
Enone	C ₆ H ₇ F ₃ O ₂	168.11	-	-	144-146 ^b 68.0 ^c
[BMIM][BF ₄]	C ₈ H ₁₅ BF ₄ N ₂	226.02	1.21	-	-
Product	C ₁₁ H ₆ F ₈ N ₂ O	334.17	-	130-131	-

^aAt 25 °C. ^b760 Torr. ^c20 Torr.¹²

Table SM 4.1.3.1.2. Summary of the utilized tools.⁹

Atom Economy (AE)	Reaction Mass Efficiency (RME)	E- factor
Ratio of the molecular weight of the desired product by the sum of molecular weights of all reactants involved in the reaction.	Percentage of the mass of the reactants that remains in the product. All reactants, yields and AE are considered.	Ratio of the generated waste weight and the total weight of the end product. Solvents and drying agents are also considered.

Table SM 4.1.3.1.3. Obtained AE and RME values in both methods.

Entry	Solvent Free/MW			[BMIM][BF ₄]/conventional thermal heating	
	AE (%)	Yield (%) ^a	RME (%)	Yield (%) ^a	RME (%)
Martins et al. (2013) ⁹	91	82 - 94	77 ^b	74- 83	61 ^c
Undergraduate student	91	81	66	83	69

^aIsolated Product. ^bat 94 % yield. ^cat 74 % yield.

Table SM 4.1.3.1.4. Obtained E-factor values in both methods.

Entry	Solvent Free/MW				[BMIM][BF ₄]/conventional thermal heating		
	Yield (%) ^a	SYS	SYS + PIS	SYS + PIS + PPS	Yield (%) ^a	SYS	SYS + PIS
Martins et al. (2013) ⁹	82 - 94	0.29 ^b	124.8 ^b	250.6 ^b	74 - 83	0.64 ^c	84.30 ^c
Undergraduate student	80.49	0.51	146.5	292.6	83.0	0.46	75.18

^aIsolated Product. ^bat 94 % yield. ^cat 74 % yield.

Characterization data⁹

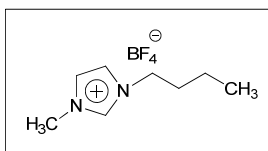
3-Methyl-1-(pentafluorophenyl)-5-(trifluoromethyl)-4,5-dihydro-5-hydroxy-1H-pyrazole (or 1-(pentafluorophenyl)-4,5-dihydro-1H-pyrazole) (C₁₁H₆F₈N₂O).

Yield: 82 - 94 % (MW), 74 - 83 % (Conventional thermal heating). Melting Point: 130 - 131 °C. ¹H NMR (CDCl₃, 600 MHz): δ, 2.09 (s, 3H, H7), 3.05 (d, 1H, ²J = 18.5 Hz, H4), 3.42 (d, 1H, ²J = 18.5 Hz, H4') ppm. ¹³C NMR ((CD₃)₂CO, 150 MHz): δ, 15.38 (C7), 47.13 (C4), 93.15 (q, ²J = 32.98 Hz, C5), 121.71 (q, ¹J = 284.81 Hz, CF₃), 147.22, 145.52, 142.22, 140.53, 138.48, 136.81 (PhF₅), 150.38 (C3) ppm; MS (EI, 70 eV): m/z (%) = 334 (M⁺, 30), 317 (10), 265 (100), 98 (1).

How to prepare a NMR sample for analysis

1. Place 0.020 g (20 mg) of the product (M3) into an NMR tube.
2. Add 600 μL of CDCl₃ (containing TMS as an internal reference) to the NMR tube.
3. Acquire the ¹H NMR and ¹³C NMR spectra.
4. If necessary, recrystallize the product with 60 mL of hexane and repeat the analysis.

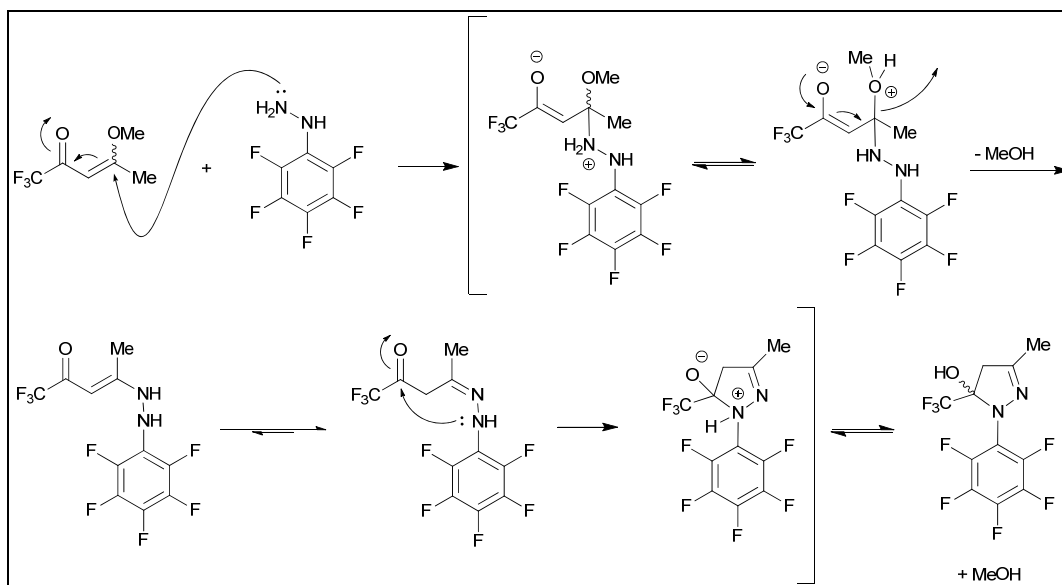
Schemes



Scheme SM 4.1.3.1.1. Structure of 1-Butyl-3-methylimidazolium tetrafluoroborate ([BMIM][BF₄] - IL).

Reaction Mechanism

In the **Scheme SM 4.1.3.1.2** is shown a proposed mechanism for synthesis of 1-(pentafluorophenyl)-4,5-dihydro-1*H*-pyrazoles.

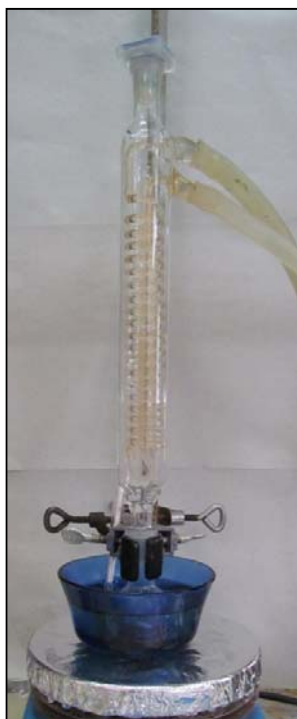


Scheme SM 4.1.3.1.2. Proposed mechanism for the reaction, same concept presented by Martins (2008).¹⁰

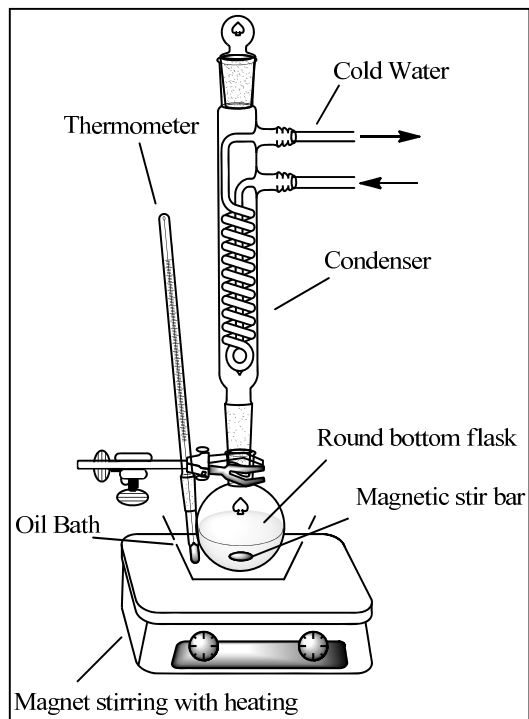
Figures

Photos of the experiment

Conventional Method:

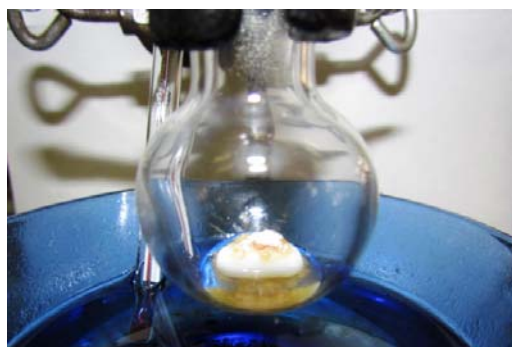


(a)



(b)

Figure SM 4.1.3.1.1. Photo (a) and scheme (b) of the system used for the synthesis in the traditional method.



(a)



(b)

Figure SM 4.1.3.1.2. Round-bottom flask before (a) and after (b) the conventional reaction.

MW Method:



Figure SM 4.1.3.1.3. MW apparatus.

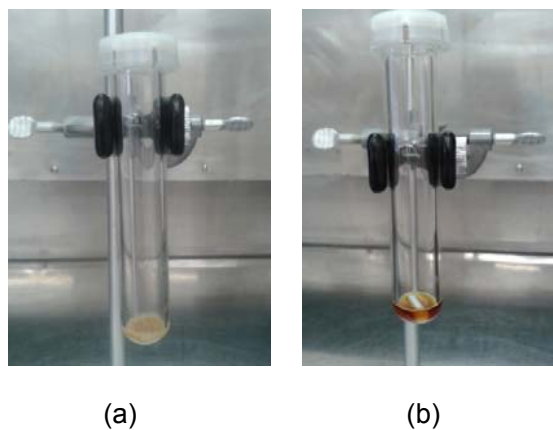


Figure SM 4.1.3.1.4. Flask before (a) and after (b) the MW reaction.



Figure SM 4.1.3.1.5. Final Product (MW method).

General Procedure

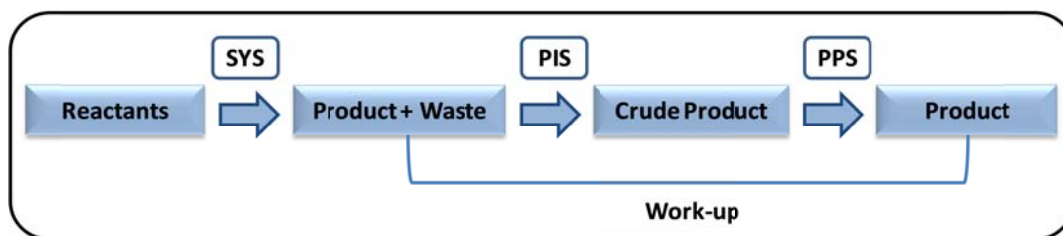


Figure SM 4.1.3.1.6. Procedure to obtain products: synthesis step (SYS), product isolation steps (PIS), and product purification step (PPS). Adapted from Martins et al. (2013) with kind permission from Springer Science and Business Media.⁹

^1H and ^{13}C NMR spectra

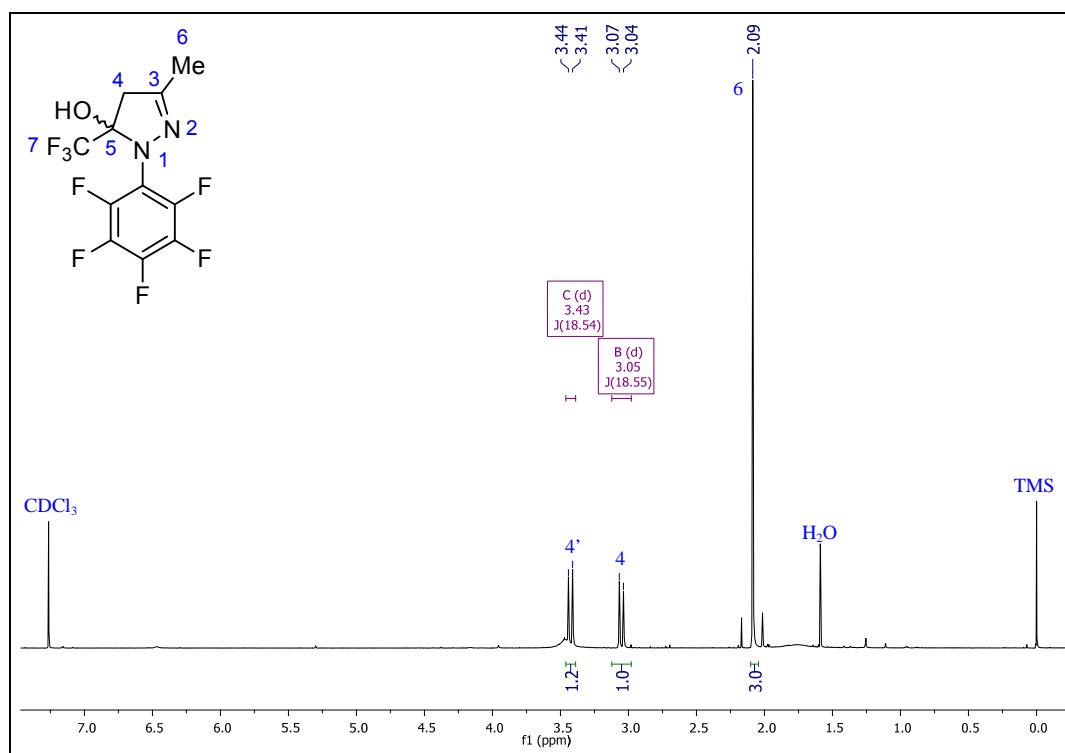


Figure SM 4.1.3.1.7. ^1H NMR spectrum (600 MHz; CDCl_3 ; 25 °C) of 1-(pentafluorophenyl)-4,5-dihydro-1H-pyrazole.

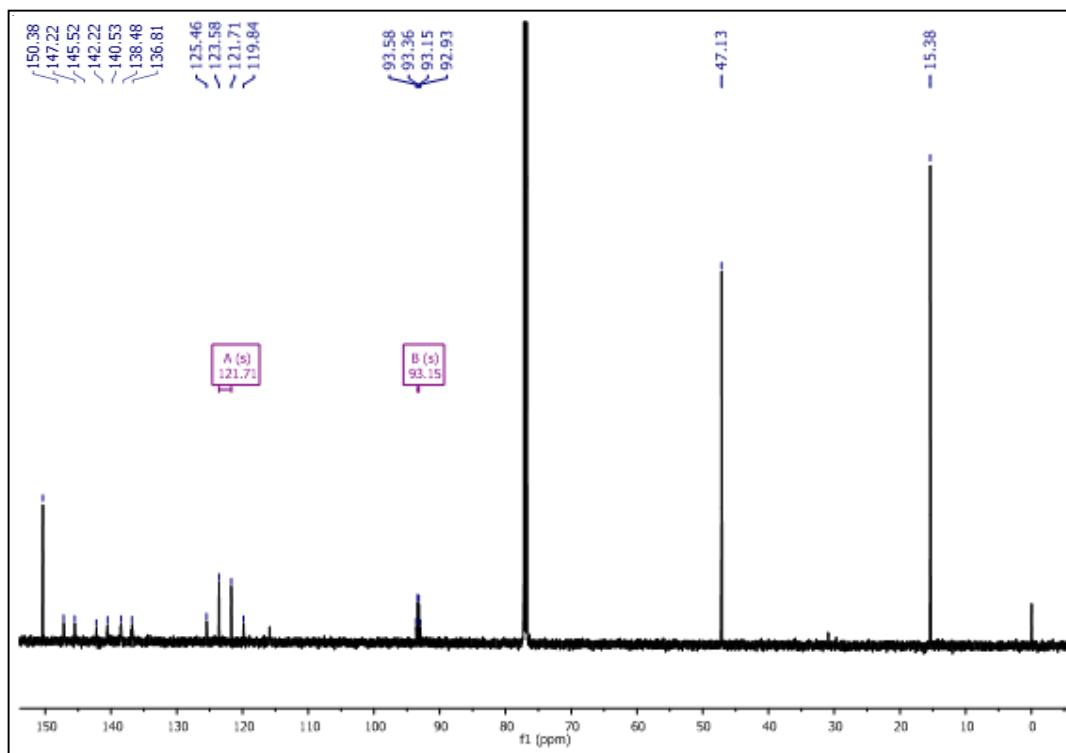


Figure SM 4.1.3.1.8. ^{13}C NMR spectrum (150 MHz; CDCl_3 ; 25 °C) of 1-(pentafluorophenyl)-4,5-dihydro-1*H*-pyrazole.

CG-MS spectra

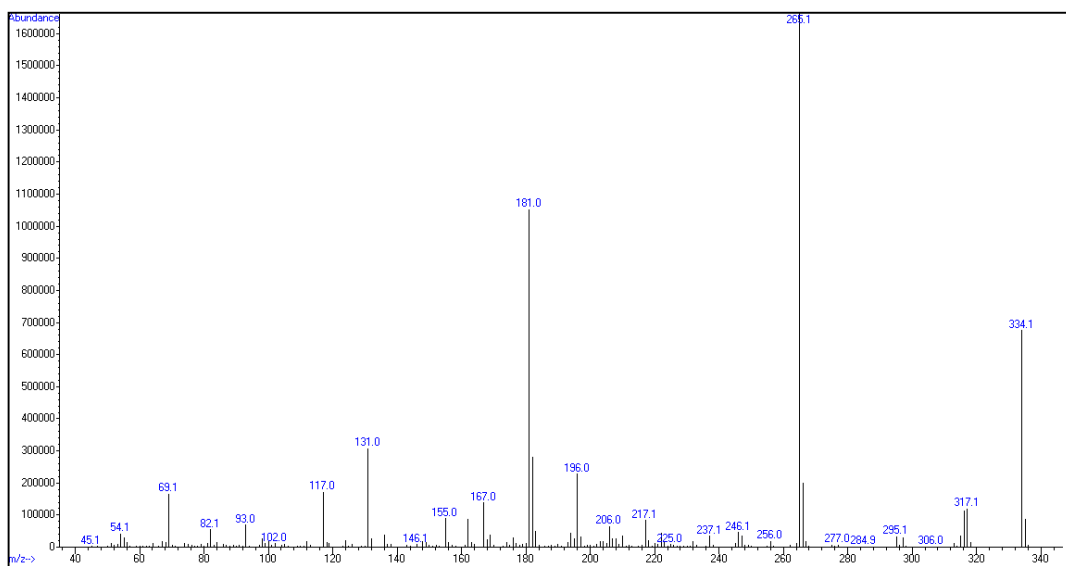


Figure SM 4.1.3.1.9. CG-MS spectrum of 1-(pentafluorophenyl)-4,5-dihydro-1*H*-pyrazole.

Thermal Analysis

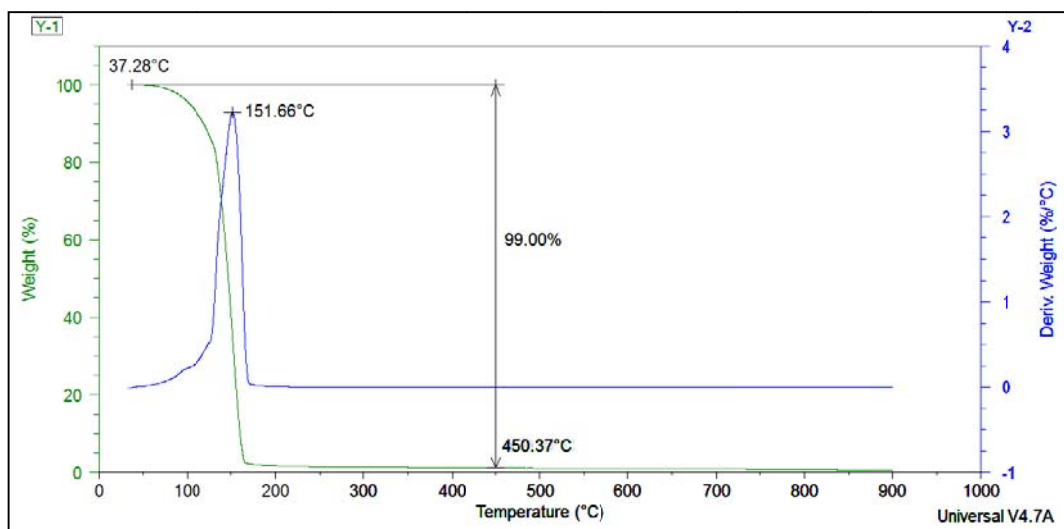


Figure SM 4.1.3.1.10. Thermogravimetric analysis (TGA) of 1-(pentafluorophenyl)-4,5-dihydro-1*H*-pyrazol.

Schematic conclusions

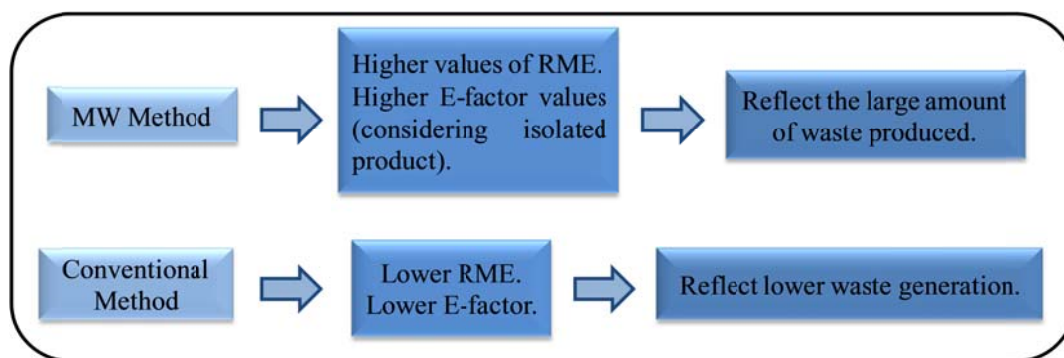


Figure SM 4.1.3.1.11. Schematic conclusion about the waste generation in the experiment.⁹

-
- ¹ C.P. Frizzo, M.R.B. Marzari, L. Buriol, D.N. Moreira, F.A. Rosa, P.S. Vargas, N. Zanatta, H.G. Bonacorso, M.A.P. Martins. *Catal Commun.* 2009, **10**, 1967.
- ² M.A.P. Martins, W. Cunico, C.M.P. Pereira, A.F.C. Flores, H.G. Bonacorso, N. Zanatta. *Curr Org Synth.* 2004, **1**, 391.
- ³ K. Alfonsi, J. Colberg, P.J. Dunn, T. Fevig, S. Jennings, T.A. Johnson, H.P. Kleine, C. Knight, M.A. Nagy, D.A. Perry, M. Stefaniak. *Green Chem.* 2008, **10**, 31.
- ⁴ D. Kralisch, A. Stark, S. Korsten, B. Ondruschka, G. Kreisel. *Green Chem.* 2005, **7**, 301.
- ⁵ D.J.C. Constable, A.D. Curzons, V.L. Cunningham. *Green Chem.* 2002, **4**, 521.
- ⁶ R.A. Sheldon. *J Chem Technol Biotechnol.* 1997, **68**, 381.
- ⁷ P.J. Dunn, S. Galvin, K. Hettenbach. *Green Chem.* 2004, **6**, 43.
- ⁸ M.A.P. Martins, C.P. Frizzo, D.N. Moreira, L. Buriol, P. Machado. *Chem Rev.* 2009, **109**, 4140.
- ⁹ M.A.P. Martins, P.H. Beck, L. Buriol, C.P. Frizzo, D.N. Moreira, M.R.B. Marzari, M. Zanatta, P. Machado, N. Zanatta, H.G. Bonacorso. *Monatsh Chem.* 2013, **144**, 1043.
- ¹⁰ M.A.P. Martins, D.N. Moreira, C.P. Frizzo, K. Longhi, N. Zanatta, H.G. Bonacorso. *J. Braz. Chem. Soc.* 2008, **19**, 1361.
- ¹¹ R. W. Lang, *Helvetica Chimica Acta.* 1988, **71**, 596.
- ¹² M. Hojo. *Synthesis.* 1986, **12**, 1013.

Cyclocondensation reaction in a Ball Mill, Grinding and Conventional Thermal Heating

Supplementary Material

Experimental Notes	1
Table of results of experiments.....	4
Physical Properties.....	4
General Data.....	4
Reaction Mechanism.....	5
Figures	
Photos of the Experiment.....	5
¹ H and ¹³ C NMR spectra.....	7
GC-MS spectra.....	8
Thermal Analysis.....	8

- The experiment proposed describes the synthesis of NH-pyrazoles from the reaction of enaminone and hydrazine hydrochloride in solid state using *p*-toluenesulfonic acid (TsOH) as a catalyst. The reaction was performed on grinding, ball mill and, conventional thermal heating. The two first methods are in solvent-free conditions. All the reactants can be commercially obtained. Enaminone also can be obtained by experimental procedures described by Martins *et. al.*^{1,2}
- Two different mechanochemical methods are employed: grinding and ball mill (**Figure SM 4.1.3.2.1**). Some reactions without solvent (e.g. using mechanochemical methods) which involve macroscopic organic solids, occur through a molten or liquid phase (melt phase). This liquid phase is probably due to the formation of high thermal energy regions (hot spots) generated by collisions between the reactants in the milling process.^{1,2} The theory of hot spots is related to high temperatures (~1000 °C) at shorter times (between 10⁻⁴ and 10⁻³ s⁻¹).³ Some studies performed in different organic reactions, identified that the liquid phase corresponds to the existence of a eutectic mixture, which occurs when the melting mixture temperature is below the melting point of each reagent.^{3,4}

- In the ball mill method, the product formation went through a liquid phase, which is probably related to the melt phase (**Figure SM 4.1.3.2.2d**).⁵ The reaction performed without TsOH resulted in 0 % conversion and, therefore, it is possible to confirm that there is no liquid phase without TsOH (**Figure SM 4.1.3.2.2a**). Additionally, the liquid phase was not observed in the milling of hydrazine hydrochloride and TsOH (**Figure SM 4.1.3.2.2b**). On the other hand, the observation of a liquid phase during the formation of products is detected in the reaction between enaminone and TsOH (**Figure SM 4.1.3.2.2c**), indicating that the melt phase in this reaction is binary and occurs due to the mixture of these reactants. In this experiment, the formation of a liquid phase was confirmed by differential scanning calorimetry (DSC) experiments. DSC results show that all mixtures have a melting point lower than the melting point of the pure separated reagents (see **Figures SM 4.1.3.2.8 - SM 4.1.3.2.10**). The same melt phase can be observed in the grinding method.
- When the experiment was conducted by an undergraduate student, was achieved around 86 % of isolated yield in 6 min of reaction (grinding), 80 % in 3 min (ball mill), 75 % in 2 h (oil bath) for methods A, B and C, respectively. The students need to have, as pre-requisite, a basic organic chemistry class. **Figure SM 4.1.3.2.3** demonstrates the reaction at different stages using a ceramic mortar and pestle. Before and at the beginning of the reaction, all the reactants are in the solid state (**Figure SM 4.1.3.2.3a** and **SM 4.1.3.2.3b**). After 45 seconds, formation of a melt phase is observed (**Figure SM 4.1.3.2.3c**). At the end (before the isolation process), the reaction mixture is in the melt form (**Figure SM 4.1.3.2.3d**).
- Another type of mortar and pestle material also can be used. If a mortar and pestle of agate is used, the reaction occurs with the same steps and shows the same aspects (**Figure SM 4.1.3.2.4**). However, there is a difference in reaction time. After 6 minutes, the conversion of reactants to products is not complete (90 % of conversion), and full conversion is only observed at 8 minutes. This behavior can be explained by the fact that the agate material presents less friction between mortar/pestle and

reactants when compared with ceramic mortar and pestle. It is important to mention that the reaction can be performed at different scales in all methods. However, the molar proportions should be maintained.

- The mechanism of 1*H*-pyrazole formation involves a cyclocondensation reaction. The enaminone (**1**) has two electrophilic centers (C1 and C3) capable of undergoing a nucleophilic attack by hydrazine (**2**). The proposed mechanism for the product formation is presented in **Scheme SM 4.1.3.2.1**. The Bronsted acid (TsOH) protonates the carbonyl oxygen, increasing the electrophilicity of C3. Thus, the attack is favored at C3 in the first stage of the reaction and the nucleophilic attack of the nitrogen atoms of hydrazine occurs in the β -carbon of enaminone (**I**). When the oxygen charge returns -NMe₂ is lost as HNMe₂ (**II**), forming enamine (**IIIa**). In this step, the imine-enamine equilibrium is shifted toward imine (**IIIb**), which is the more reactive species. Then, the carbonyl group of β -enaminone undergoes the N nucleophilic attack, reaching a new transition state (**IV**). The H₂O elimination leads to the final product (**3**) which may be in its tautomeric form.⁶ The hydrazine can be used in a little excess to ensure that all enaminone will be consumed. This reaction also can be performed under conventional thermal heating method, using ethanol as solvent. However, this process requires more steps, thus generating more waste.

- The ¹H-NMR and ¹³C-NMR of 5(3)-Phenyl-1*H*-pyrazole are shown in **Figures SM 4.1.3.2.5** and **SM 4.1.3.2.6**. In the ¹H-NMR, it is possible to observe the signals of vinyl hydrogen atoms of the pyrazole ring (H3 and H4) and the signals of aromatic hydrogen atoms. In the ¹³C-NMR, besides the vinyl carbons of pyrazole and aromatic carbons, the C directly bound to the aromatic ring (C5) is observed. **Figure SM 4.1.3.2.7** shows the CG-MS spectra of the final product.

Table SM 4.1.3.2.1. Solvent-free experiments conducted in a grinding, ball mill and oil bath method, using enaminone **1** and hydrazine **2** as started materials and TsOH as catalyst.

Entry	Method	Solvent	Temperature (°C)	Reaction Time (min)	Isolated Yield (%) ^d	Melting Point (°C)
1 ^a	ball mill	-	-	3	75-80	69-71
2 ^b	grinding	-	-	6	85-90	69-71
3 ^c	oil bath	ethanol	80	120	74-79	69-71

^a Reaction conditions: 3 mmol of enaminone, 3.6 mmol of hydrazine, 10 mol% of TsOH, steel beaker (25 mL), steel milling balls (5 mm x 10 mm), and 450 rpm. ^b Reactions conditions: 1 mmol of enaminone, 1.2 mmol of hydrazine, and 20 mol% of TsOH. ^c Reaction conditions: 1 mmol of enaminone, 1.2 mmol of hydrazine, and 20 mol% of TsOH. ^d The compounds are dissolved in water and extracted with CHCl₃ (3 × 20 mL).

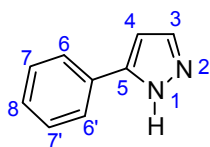
Physical Properties of reactants and product

Table SM 4.1.3.2.2. Physical properties of chemical compounds used in the experiment.

Compound	Chemical formula	Molecular mass (g·mol ⁻¹)	Density (g·cm ⁻³) ^a	Melting point (°C)	Boiling point (°C)	Refractive Index
Enaminone 1	C ₁₁ H ₁₃ NO	175.23	-	91	-	-
Hydrazine 2	H ₅ N ₂ Cl	68.51	-	89	-	-
Pyrazole 3	C ₄ H ₅ N ₂	77.07	-	69-71	-	-
TsOH	C ₇ H ₈ O ₃ S	172.20	-	103-106	-	-
Sodium sulfate	Na ₂ SO ₄	142.04	2.68	884	-	-
Chloroform	CHCl ₃	119.38	1.49	-63	60-61	1.450
Ethanol	C ₂ H ₅ OH	46.07	0.79	-114	78.37	1.360

^aAt 25 °C.

General data

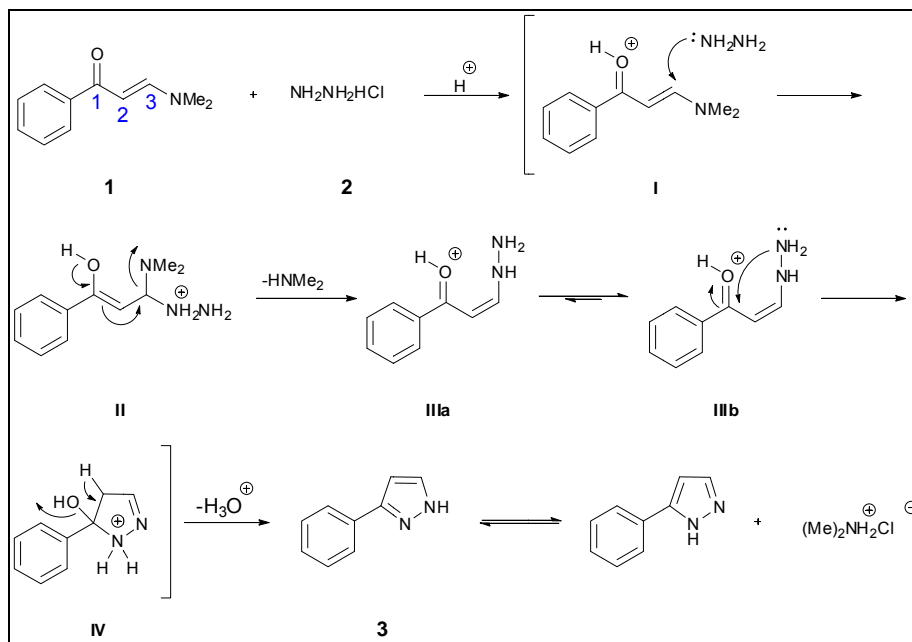


5(3)-Phenyl-1H-pyrazole.

Yellow solid. **Melting Point:** 69 - 71 °C. **¹H NMR:** (200 MHz, CDCl₃) δ, 6.62 (d, ³J = 1.40 Hz, 1 H, H4), 7.34-7.45 (m, 3H, H-Arom), 7.61 (d, ³J = 1.40 Hz, 1H, H3), 7.77-7.80 (m, 2H, H-Arom), 9.62 (br s, 1H, NH). **¹³C NMR** (50 MHz, CDCl₃) δ, 102.6 (C4), 125.9, 128.0, 128.8, 132.2 (C-Arom), 133.4 (C5), 149.0 (C3). **GC-MS** (m/z, %) 144 (M⁺, 100), 115 (20), 77 (12), 63 (7), 51 (6).

Reaction Mechanism

The Scheme **SM 4.1.3.2.1** shows the proposed mechanism for the synthesis of 1H-Pyrazole.



Scheme SM 4.1.3.2.1. Proposed mechanism for the reaction between enaminone and hydrazine.

Photos of the experiment



(a)



(b)



(c)

Figure SM 4.1.3.2.1. Images of the two mechanochemical apparatus: (a) planetary ball mill, (b) mortar and pestle (grinding) and (c) oil bath (conventional method). (b) Reproduced with permission from Martins et al., *ACS Sustainable Chem. Eng.*, 2014, 2, 1895-1899. Copyright (2014) American Chemical Society.

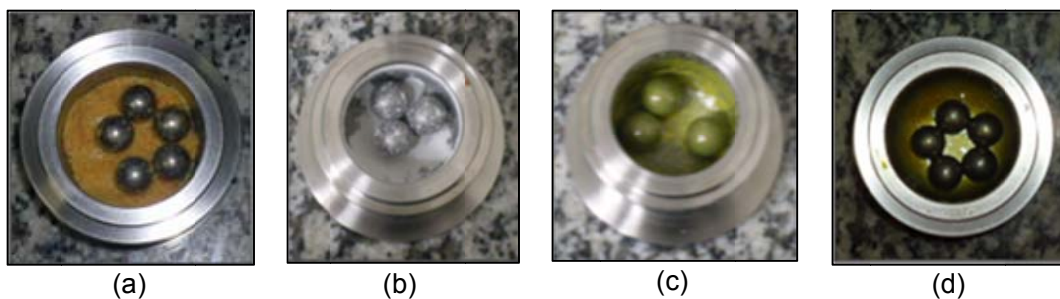


Figure SM 4.1.3.2.2. Images that demonstrate the mixture between (a) enaminone and hydrazine, (b) hydrazine and TsOH, (c) enaminone and TsOH (melt phase) and (d) hydrazine, enaminone and TsOH (melt phase), in a planetary ball mill.

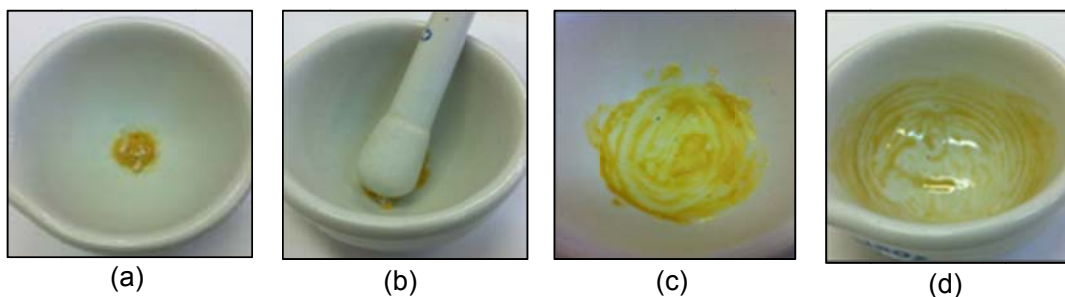


Figure SM 4.1.3.2.3. The mixture of enaminone, hydrazine and TsOH in ceramic grinding, (a) before the reaction, (b) at the beginning, (c) when the melt phase is formed and (d) at the end of the reaction.

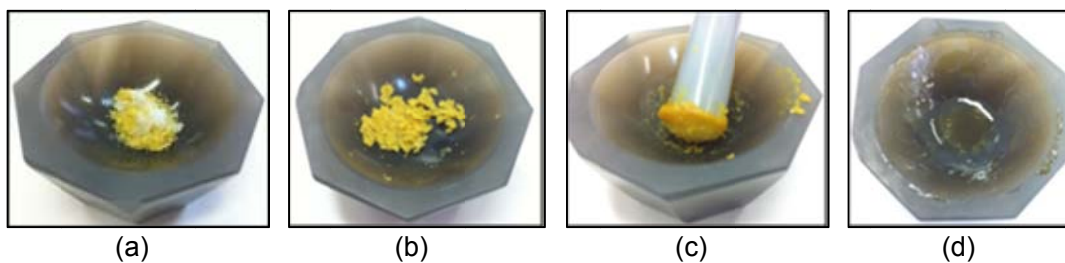


Figure SM 4.1.3.2.4. The mixture of enaminone, hydrazine and TsOH in agate grinding: (a) before the reaction, (b) at the beginning, (c) when the melt phase is formed and (d) at the end of the reaction.

^1H and ^{13}C NMR spectra

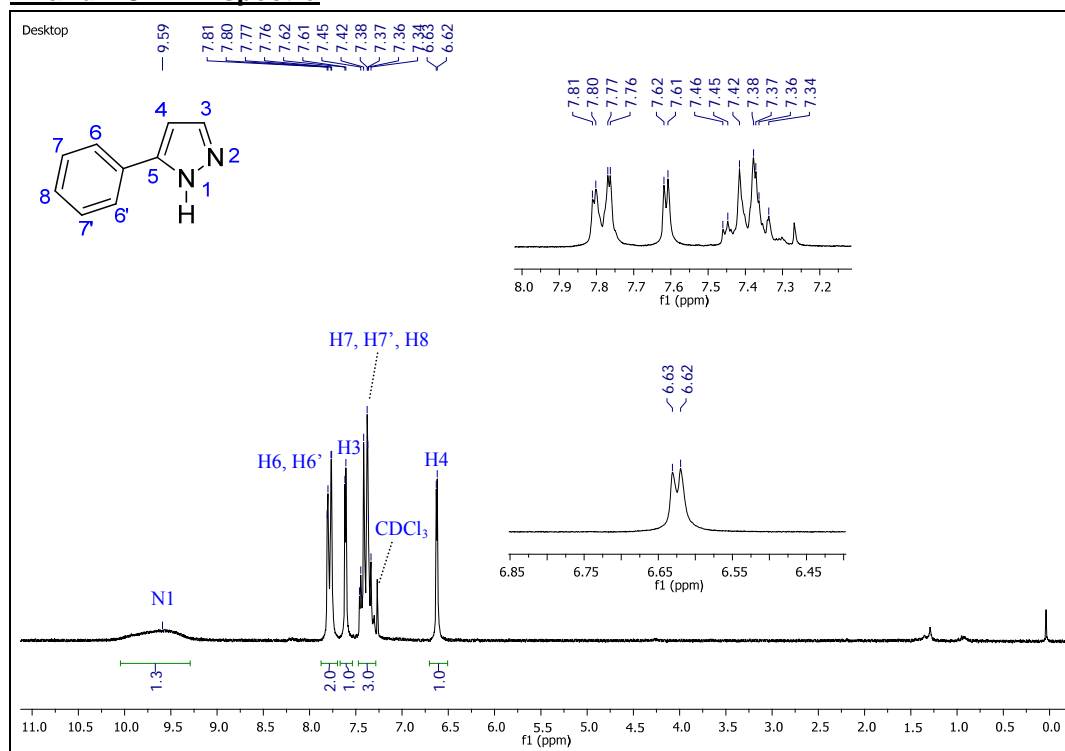


Figure SM 4.1.3.2.5. ^1H NMR spectrum (200 MHz, CDCl_3 , 25 °C) of 5(3)-Phenyl-1H-pyrazole.

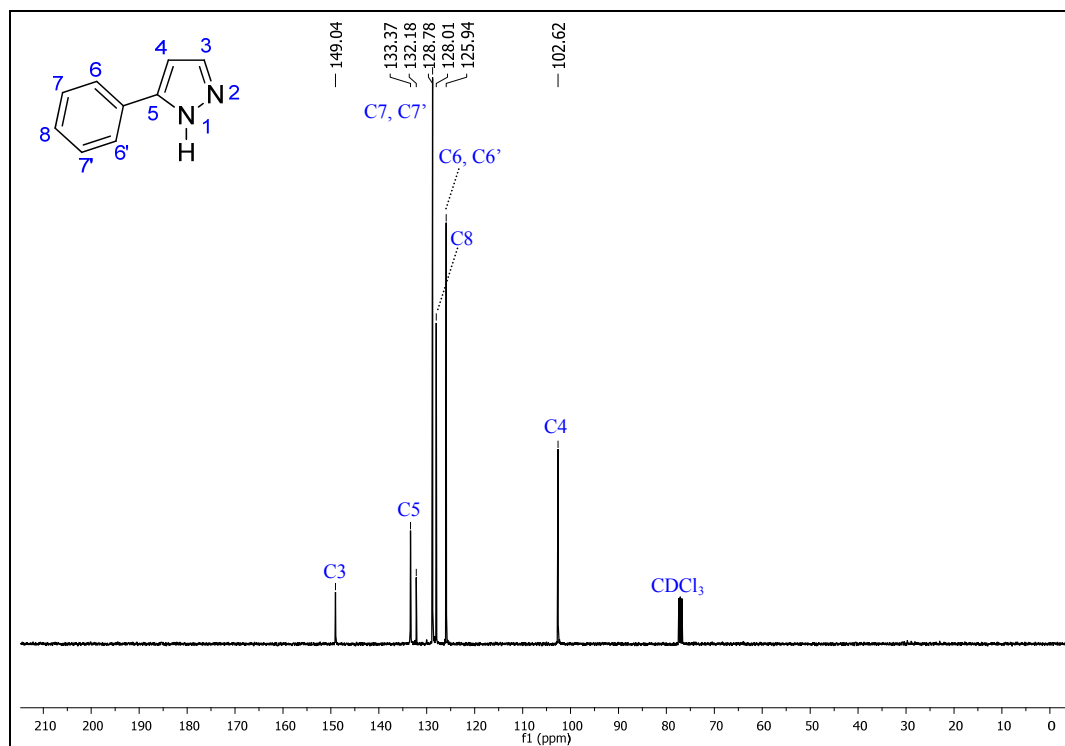


Figure SM 4.1.3.2.6. ^{13}C NMR spectrum (50 MHz, CDCl_3 , 25 °C) of 5(3)-Phenyl-1H-pyrazole.

GC-MS spectra

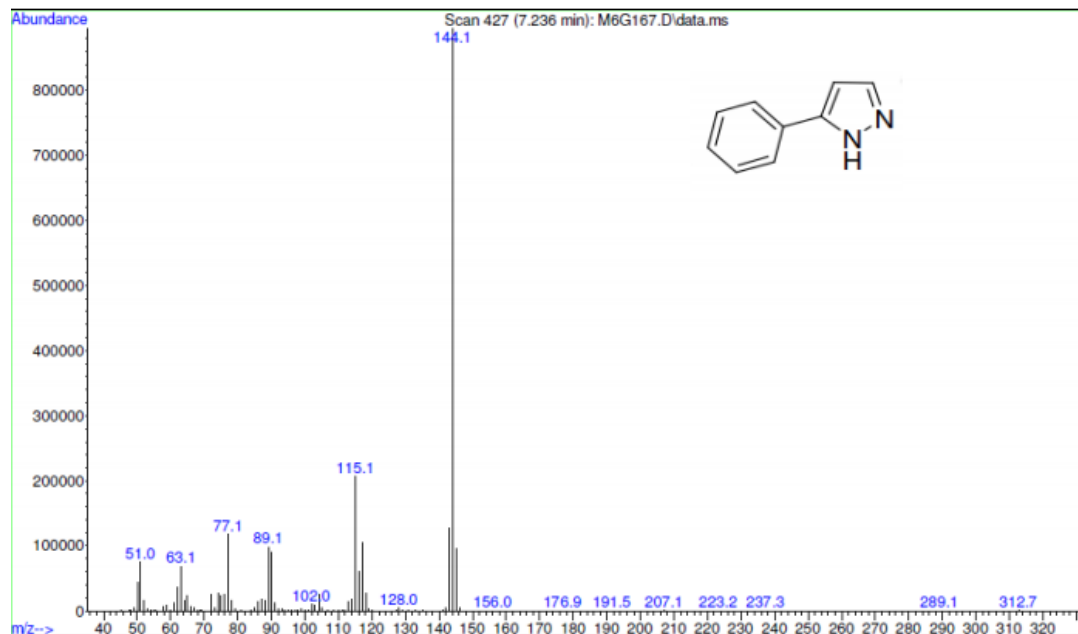


Figure SM 4.1.3.2.7. GC-MS spectrum of 5(3)-Phenyl-1H-pyrazole.

Thermal Analysis

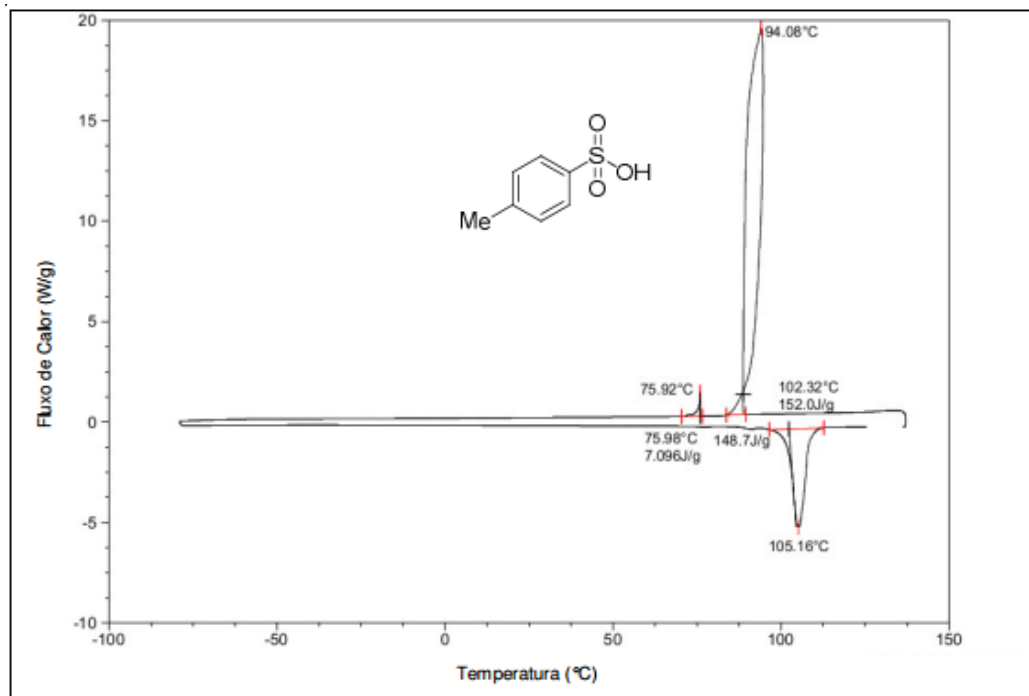


Figure SM 4.1.3.2.8. Thermal analysis of TsOH obtained by DSC (heating rate of 10 °C·min⁻¹).

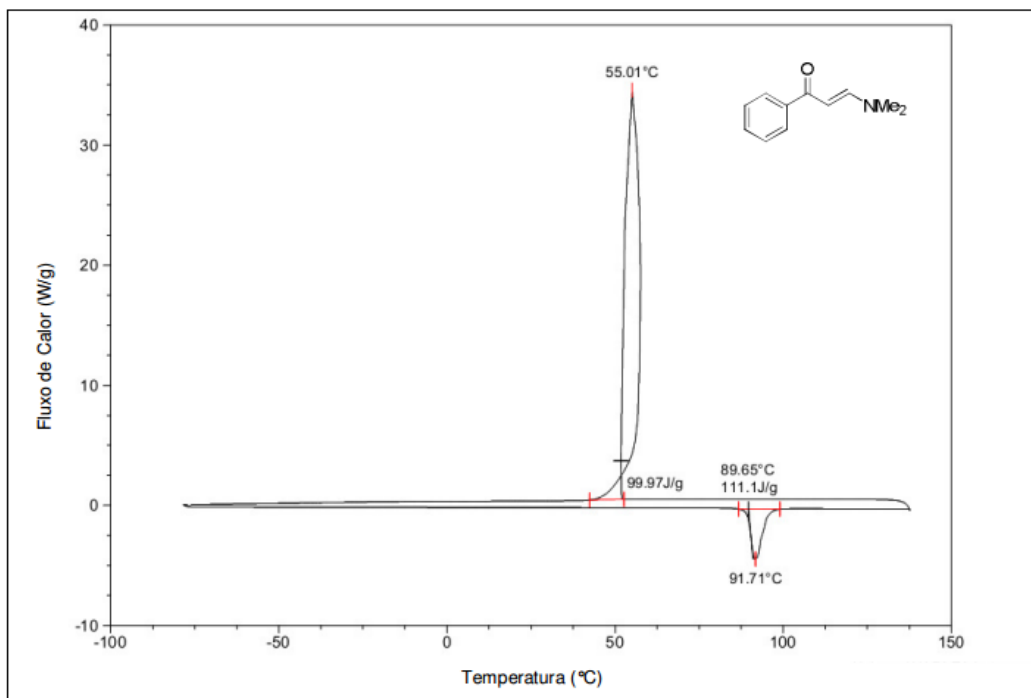


Figure SM 4.1.3.2.9. Thermal analysis of enaminone obtained by DSC (heating rate of $10\text{ }^{\circ}\text{C}\cdot\text{min}^{-1}$).

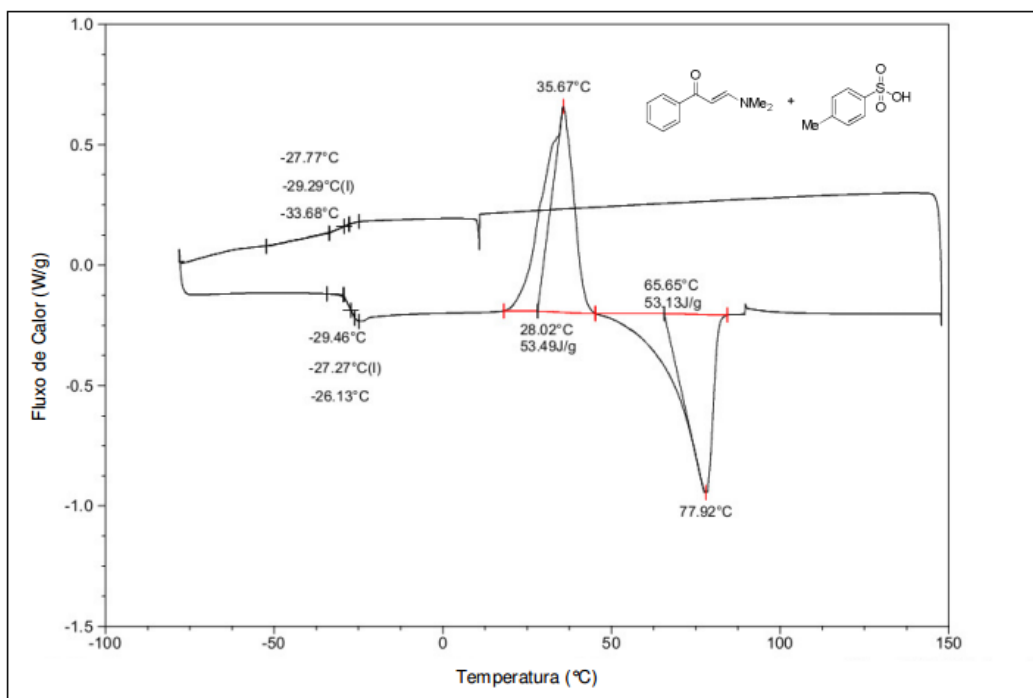


Figure SM 4.1.3.2.10. DSC analysis of TsOH and enaminone mixture confirms the formation of a binary melt phase between these reactants (heating rate of $10\text{ }^{\circ}\text{C}\cdot\text{min}^{-1}$).

- ¹ M.A.P. Martins, C.P. Frizzo, D.N. Moreira, F.A. Rosa, M.R.B. Marzari, N. Zanatta, H.G. Bonacorso. *Catal. Commun.* 2008, **9**, 1375.
- ² F.A. Rosa, P. Machado, H.G. Bonacorso, N. Zanatta, M.A.P. Martins. *J. Heterocycl. Chem.* 2008, **45**, 879.
- ³ E. Boldyreva. *Chem. Soc. Rev.* 2013, **42**, 7719.
- ⁴ P. Nun, C. Martin, J. Martinez, F. Lamaty. *Tetrahedron.* 2011, **67**, 8187.
- ⁵ S.L. James, C.J. Adams, C. Bolm, D. Braga, P. Collier, T. Friciú , F. Grepioni, K.D.M. Harris, G. Hyett, W. Jones, A. Krebs, J. Mack, L. Maini, A.G. Orpen, I.P. Parkin, W.C. Shearouse, J.W. Steed, D.C. Wadell. *Chem. Soc. Rev.* 2012, **41**, 413.
- ⁶ F.A. Rosa, P. Machado, H.G. Bonacorso, N. Zanatta, M.A.P. Martins, *J. Heterocycl. Chem.* 2008, **45**, 879.

Organocatalytic enantioselective Michael addition of thiophenol to chalcone

Supplementary Material

The main purpose of this experiment is to illustrate the use of organocatalytic enantioselective Michael addition reaction and enantiomeric enrichment by crystallization as a remarkable tool for easy preparation of optically pure compounds. An important aspect is also the formation of new carbon-sulfur bonds in a simple experiment. The obtained chiral adduct can be readily transformed into different classes of organic compounds.

The student body is students of advanced organic chemistry, who have theoretical knowledge of the mechanism of C-S bond formation in the Michael addition, and methods of optical resolution of enantiomeric mixtures. The students should be skilled enough to perform the reaction and obtain the enantioenriched product by crystallization.

The experiment was performed on a 10-mmol scale and the repeatability of the experiment was confirmed by 2nd year undergraduate students.

Additional notes on the preparation of (+)-(R)-3-phenylsulfanyl-1,3-diphenylpropan-1-one: The reaction was run with 1.5% mol of (+)-cinchonine and this catalyst was the best among tested *Cinchona* alkaloids (**Table SM 4.1.3.3.1**). The highest ee was observed for the addition at -20 °C. An increase the temperature of the process significantly reduces enantioselectivity of this reaction, and results in a decreased yield of pure enantiomer.

Table SM 4.1.3.3.1 – Results of the Michael addition of thiophenol to *trans*-chalcone

Entry	Catalyst ^a	Temperature (°C)	Yield (%)	ee (%)
1	Cinchonidine	-20	99	14
2	Quinine	-20	98	17
3	Cinchonine	-20	96	70
4	Cinchonine	0	91	38
5	Cinchonine	-70	80	50

^a Applied in a 1.5 mol% amount of catalyst, 2 mmol reaction scale in toluene.

According to this procedure, the addition product was formed in 94–99% yield and 65–75% ee. Already the first crystallization gave enantiomerically pure product in 65–70% total yield with over 98% ee. Enantiomeric excess was calculated by comparing the measured optical rotation with the literature data.^{1,2} ($[\alpha]_D^{20} = +136$ (1.02, CH₂Cl₂), extrapolated for 100% ee).

The resulting enantiomerically pure adduct is stable at room temperature for several years. The Michael addition reaction can be performed with a variety of sulfur nucleophiles, including aromatic and benzyl mercaptans.²

Laboratory session 1

There are no difficult stages of the experiment in this section. In order to simplify the procedure, an addition of the solution of thiophenol to the cooled mixture (via a syringe) can be carried out in three portions, at intervals of 5 minutes with continued cooling of the flask in a freezer. Be sure to flush the reaction mixture with nitrogen to protect thiophenol against oxidation to disulfide.

Next, the reaction mixture can be kept in the freezer (ca. -20 °C) without stirring for 24 hrs or more (till next session). Also the reaction could be performed in a cooling bath (a polystyrene box with ice and NaCl or a cryocooler) with stirring but not less than 4 hrs. The reaction progress can be monitored by TLC analysis on Merck silica gel 60 precoated plates, eluting with *tert*-BuOMe/CHCl₃/Hexane, 2.5:2.0:7.0, R_f = 0.43 (visualized with 254-nm UV lamp).

Laboratory session 2

An efficient aqueous work-up is very important in this procedure. Thus, the resulting mixture is purified by washing with aqueous solution of hydrochloric acid to remove the catalyst, which reacts with hydrochloric acid to afford the water-soluble cinchonine hydrochloride. Next, work-up with sodium hydroxide leads to the removal of an excess of thiophenol after the reaction complete. After drying the addition product is obtained as a white solid in yields usually above 94%. The measured melting point of the crude product was in the range 110–117 °C), and the optical rotation ($[\alpha]_{\text{D}}^{20} = +88-100$ (1.00, CH₂Cl₂)). The NMR spectra should be recorded in CDCl₃.

Laboratory session 3

Enantiomeric enrichment of the crude product by crystallization is an essential part of this experiment. It is important not to use too much dichloromethane for crystallization because it may disrupt the optical resolution by crystallization during this session. This process is completed after 2-3 hours in an ice bath. Crystallizing solution can be also left in the fridge for the next session. Sometimes too much crystals precipitated, and in such case can add cold n-hexane (25 mL) to a flask. Note, that crystallizes a racemic compound and the concentration of mother liquors allowed the isolation of enantiomerically pure product as a white fluffy solid, in total yields higher than 65% with over 98% ee. The determined melting point for this compound was 95–97 °C, and optical rotation ($[\alpha]_{\text{D}}^{20} = +134-137$ (1.00, CH₂Cl₂)). The racemic crystals had higher mp 118-120 °C and $[\alpha]_{\text{D}}^{20} = +18-23$ (1.00, CH₂Cl₂).³

Photos of the experiment



Figure SM 4.1.3.3.1 – Apparatus with the reaction mixture



Figure SM 4.1.3.3.2 – Enantiomerically pure product

¹H and ¹³C NMR spectra

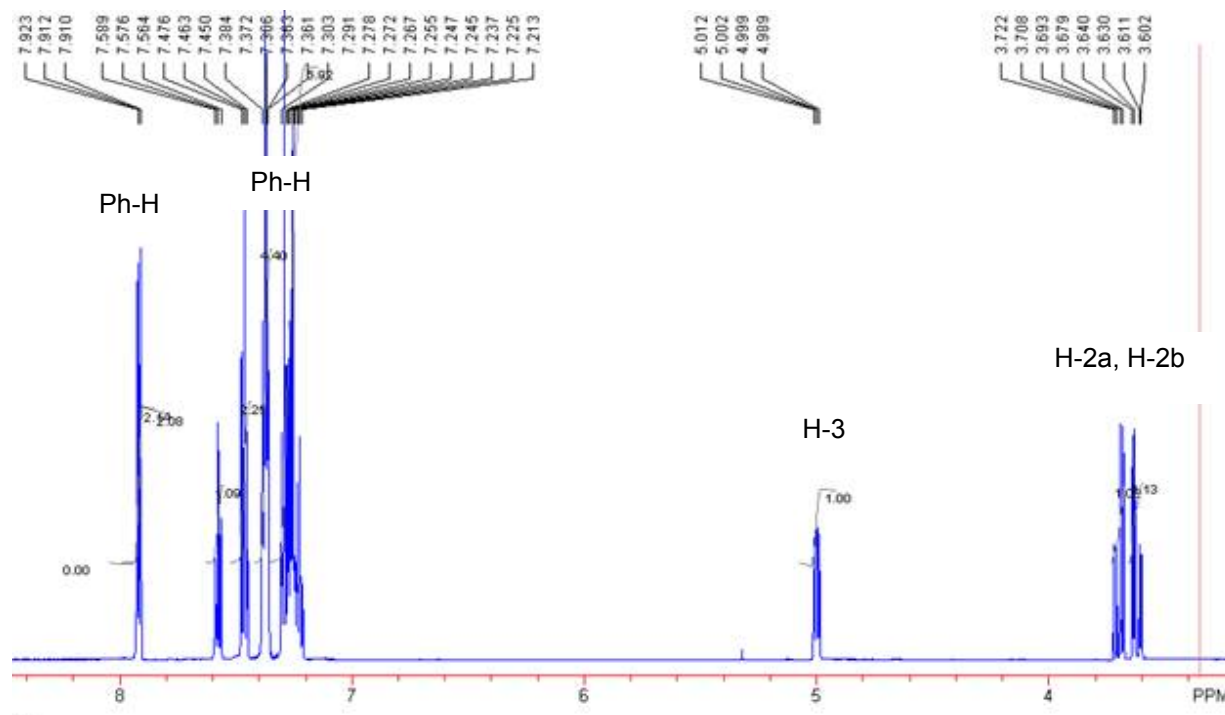


Figure SM 4.1.3.3.3 – ¹H NMR spectrum (300 MHz, CDCl₃) of (+)-(R)-3-phenylsulfonyl-1,3-diphenylpropan-1-one

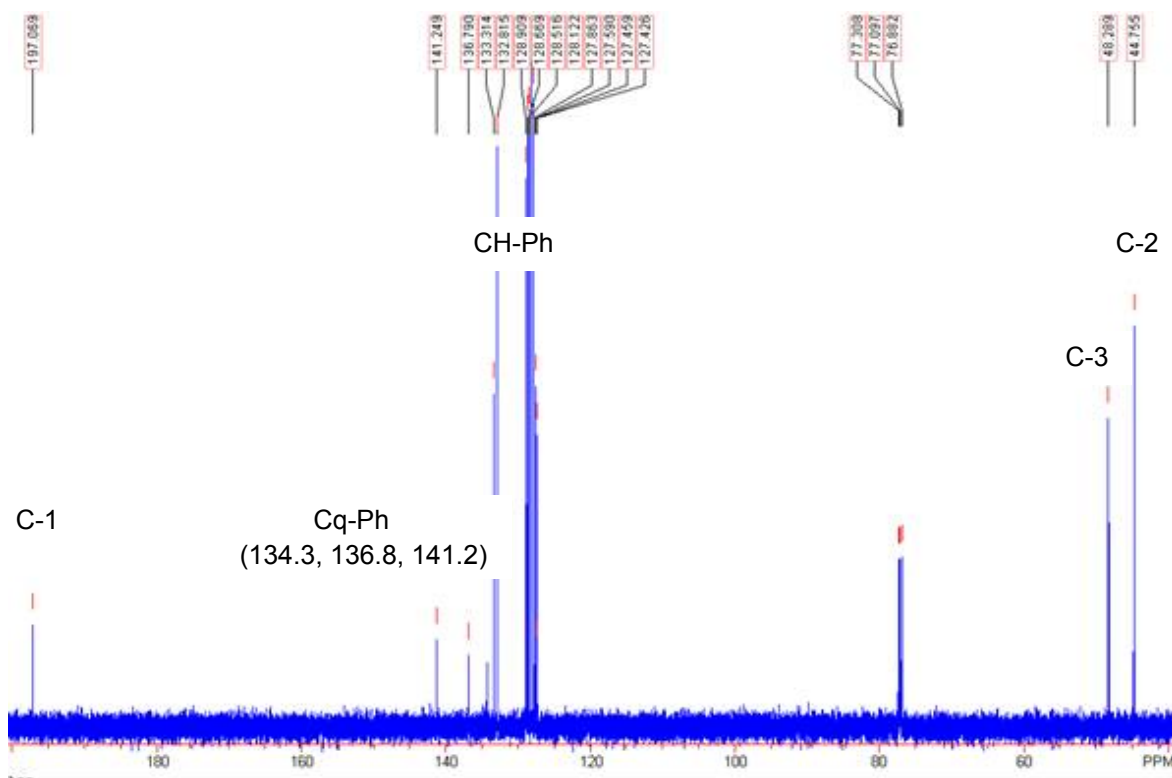


Figure SM 4.1.3.3.4 – ¹³C NMR spectrum (300 MHz, CDCl₃) of (+)-(R)-3-phenylsulfanyl-1,3-diphenylpropan-1-one

- ¹ Krotov, V. V., Staroverov, S. M., Nesterenko, P. N., Lisichkin, G. V. *J. Gen. Chem. USSR* (English Transl), 1986, **56**, 2177.
- ² Skarżewski, J.; Zielinska-Błajet, M.; Turowska-Tyrk, I. *Tetrahedron:Asymmetry*, 2001, **12**, 1923.
- ³ Katritzky, A. R., Chen, J., Belyakov, S. A. *Tetrahedron Lett.* 1996, **37**, 6631.

Stereoselective Synthesis of meso-1-allyl-2,6-diphenylpiperidin-4-one

Supplementary Information

1. Experimental notes

The main goals of this experiment is to use organocatalysis to describe a new synthesis of meso-2,6-disubstituted piperidin-4-ones by the Aza-Diels-Alder reaction between an acyclic enone, an aldehyde and an amine as a multi-component reaction, in the presence of *L*-proline as catalyst. An attractive feature of this experiment includes the one-pot, three component reaction from simple and commercially available starting materials.

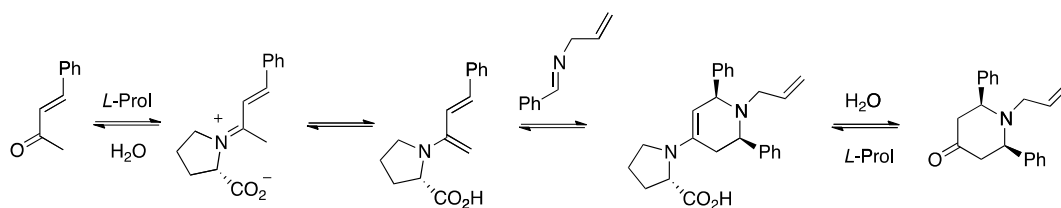
The reaction was performed in an open round bottom flask, not nitrogen was necessary. The reaction can be scale up to 3 mmol of benzaldehyde or up to multigram scale. The average yield obtained is 75-80% after chromatography column purification. The acid-base extraction is necessary to eliminate the excess of ketone (4 eq. vs 1 eq.). It is very interesting for the students to use acid-base properties for the separation of two organic compounds with different properties.

It is important to point out that the acid-base extraction has to be carried out quickly and the base solution should be cold. The piperidin-4-one are not very stable under acid conditions for long periods of time because a retro-Diels-Alder reaction would take place giving the starting materials. The pH in the basic solution should be checked (indicator paper), every time the acid aqueous solution is added.

The crude product was purified by flash silica gel 60 column chromatography (n-hexane: Ethyl acetate/ 10:1) furnishing the pure meso-2,6-diphenylpiperidin-4-one. The spot on the TLC plate can be visualized using a solution of vanillin (2.5 g of vanillin, 200 mL of EtOH, 1 mL of concentrated H₂SO₄). Do not keep the product for long time inside the column, decomposition can be produced.

This procedure has been carried out for several undergraduated students (4th year) and some graduated students for their research master degree.

2. Reaction Mechanism



Scheme SM 4.1.3.4.1. Reaction mechanism for the synthesis of *meso*-1-allyl-2,6-diphenylpiperidin-4-one.

3. Photos from the experiment

Aspect of the reaction mixture at different reaction times



Figure SM 4.1.3.4.1.

After 10 min



Figure SM 4.1.3.4.2.

After 10 h

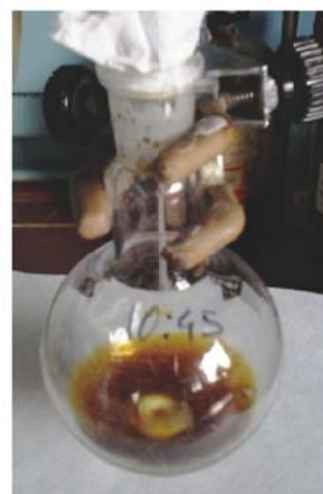
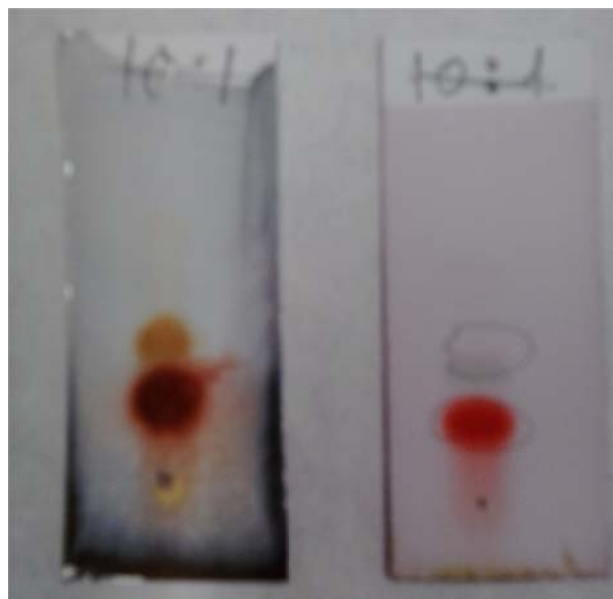


Figure SM 4.1.3.4.3.

After 24 h

4. Thin Layer Chromatography (TLC)

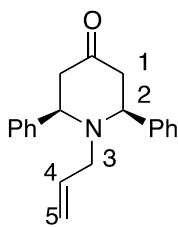


(a)

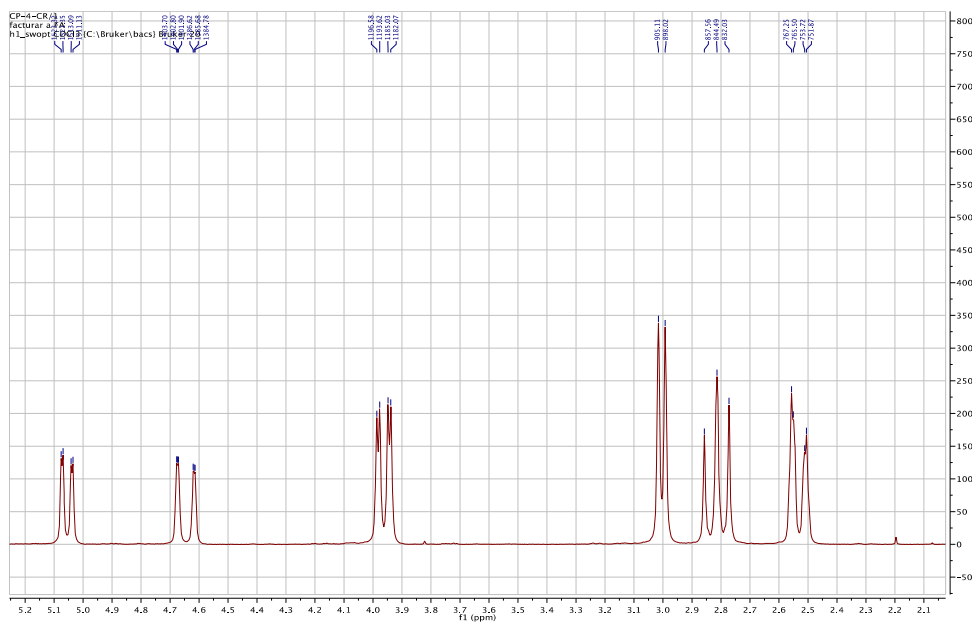
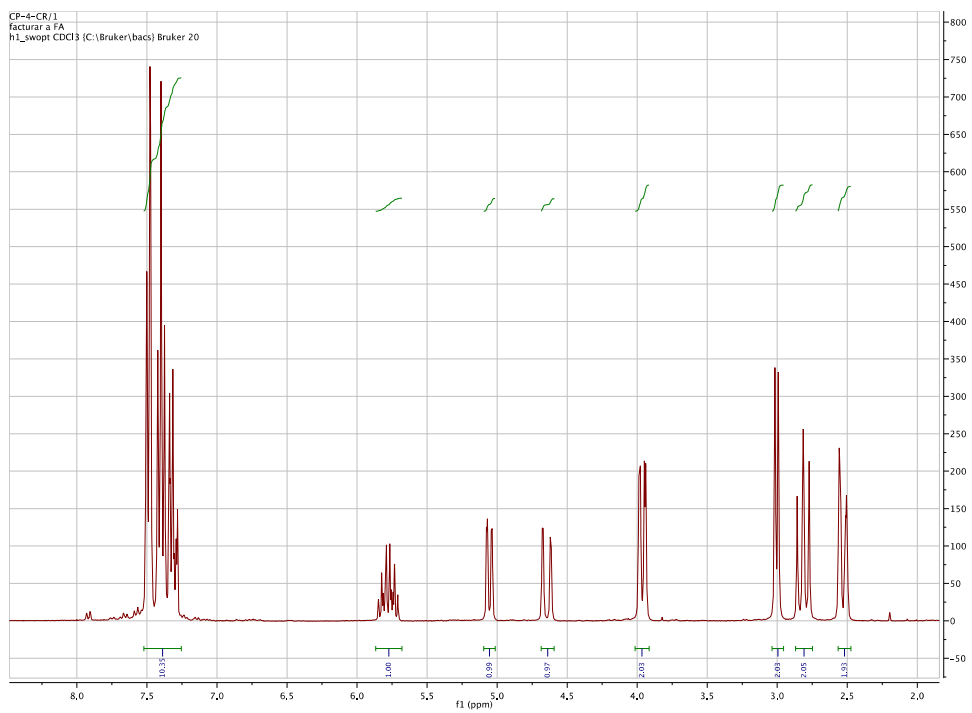
(b)

Figure SM 4.1.3.4.4. TLC (SiO_2) plates from the reaction crude mixture using a mixture of n-hexane/Ethyl Acetate; 10:1 as eluent. (a) After 24 h. of reaction; (b) after acid-base extraction.

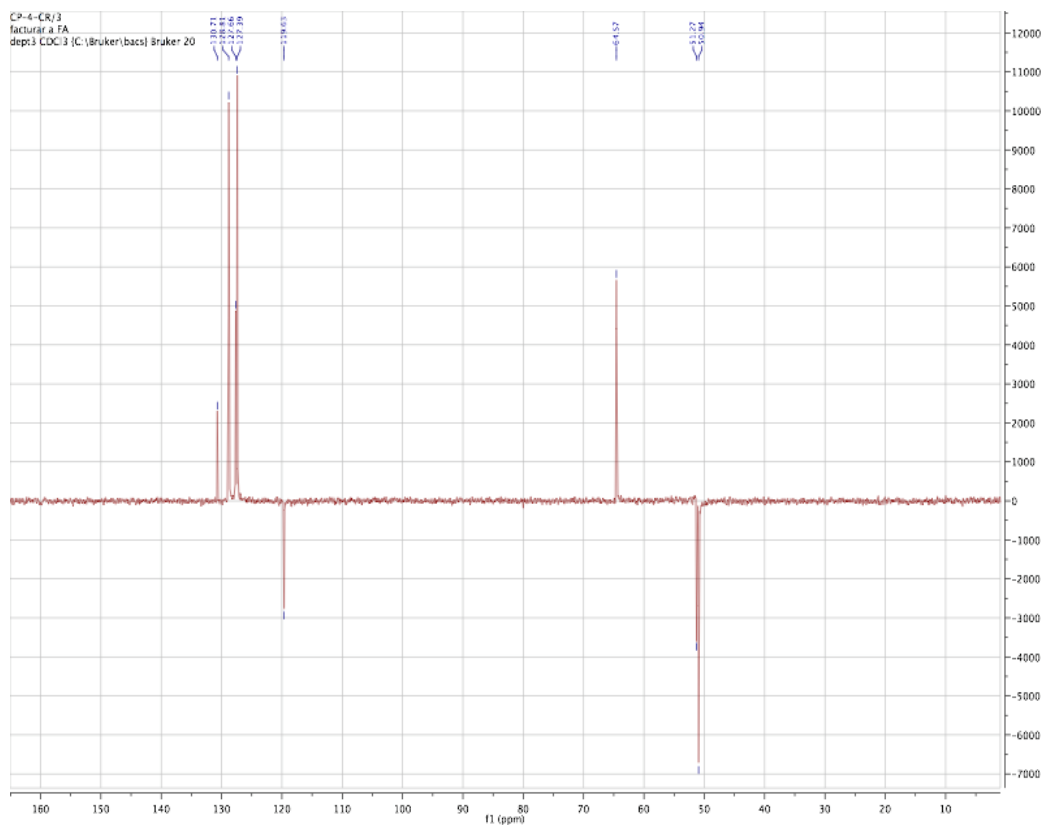
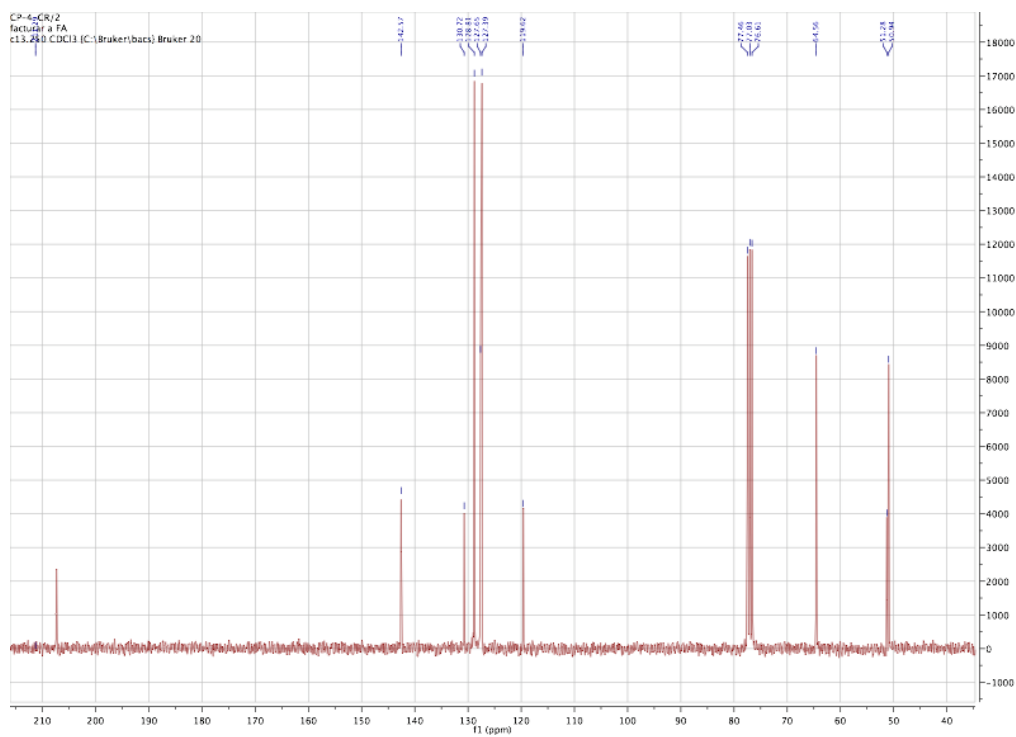
5. ¹H-NMR, ¹³C-NMR and DEPT spectra for *meso*-1-allyl-2,6-diphenylpiperidin-4-one.



¹H-RMN (CDCl₃, 300 MHz): δ(ppm)= 7.49-7.30 (m; 10H), 5.83-5.72 (m; 1H), 5.04 (dd, *J*=10.2, 2.0; 1H), 4.64 (dd, *J*=17.1, 2.0; 1H), 3.96 (dd, *J*=12.8, 2.3; 2H), 3.00 (d, *J*=7.1; 2H), 2.81 (t, *J*=12.8; 2H), 2.53 (dd, *J*=12.8, 2.3; 2H).



^{13}C -RMN (CDCl_3 , 75.4 MHz): $\delta(\text{ppm}) = 207.1$ (CO), 142.4 (2x C), 130.5 (CH), 128.6 (4x CH), 127.5 (2x CH), 127.2 (4x CH), 119.5 (CH₂), 64.4 (2x CH), 51.0 (CH₂), 50.8 (2x CH₂).



Synthesis of a squarylium cyanine dye as potential photosensitizer for PDT

Supplementary Material

Experiment Notes	1
Table of yield, m.p. and IR spectra of 3, 4 and 6 compounds.....	2
Figures	
Photo of experiment.....	2
¹ H, ¹³ C and DEPT NMR spectra.....	3

This experiment aims at the synthesis of a squarylium cyanine dye as potential photosensitizer for PDT, from a three step reaction. The first step consists in a Doebner-Miller reaction between the 4-iodoaniline and crotonaldehyde in an aqueous solution of HCl using a two-phase solvent system with toluene, and tetrabutylammonium fluoride as phase-transfer catalyst, to prepare 6-iodoquinaldine (**3**). As it is a heterogeneous reaction, it is of pivotal importance that vigorous stirring is used along this first step reaction. After work-up reaction afforded a crude 6-iodoquinaldine as a crystalline solid that is purified by recrystallization from a mixture of ethyl acetate and petroleum ether (2:1), yielding pure compound as colorless crystals with melting point 110-111 °C (Table SM 4.1.3.5.1). Nevertheless the low yield obtained (38-45%), a second crop obtained from mother liquors after evaporation and recrystallization can arise the total yield to 45-50%. This yield is similar to the reported in the literature when the product was alternatively purified by column chromatography. The two step reaction consists in the alkylation of the nitrogen atom of the 6-iodoquinaldine previously obtained with an excess (3 eq.) of 1-iodohexane in acetonitrile under reflux aims to obtain a quaternary quinaldinium salt **4**. This reaction must be let under reflux until the next session (or during a minimum of 5 days). After the mixture has cooled to room temperature the product is readily isolated by precipitation with diethyl ether. The yield of this first collection is relatively low (about 50%), but repeating twice the alkylation of the mother's liquor, yield increases to 90%. The last three step reaction consists in the squarylium cyanine dye synthesis by condensation of the quaternary quinaldinium salt **4** with squaric acid (3,4-dihydroxycyclobut-3-ene-1,2-dione) under reflux in a mixture of *n*-butanol/pyridine. As the dye is being formed, reaction mixture acquires an increasingly intense green color but the monitoring of the reaction progress is performed by TLC (silica, MeOH/CH₂Cl₂, 2%).

Structure of the obtained **3**, **4** and **6** compounds were elucidated by m.p., IR (KBr) and NMR spectroscopy (spectra obtained using 400 or 600 MHz instruments). Additionally, the Visible spectrum of dye **6** was recorded (Figure SM 4.1.3.5.8) showing a narrow and strong band within the so called

“phototherapeutic window” ($\lambda_{\max} = 707$, $\log \epsilon = 5.16$). To the best of our knowledge, dye **6** is a new recently squarylium cyanine dye bearing two iodine atoms in its structure, presenting a $m/z = 784.10057$ [M^+] (calc. $C_{36}H_{38}I_2N_2O_2$ 784.10172) determined by HRMS ESI-TOF.

Table SM 4.1.3.5.1 describes the average values of yield, m.p. and IR spectra for **3**, **4** and **6** compounds. 1H NMR, ^{13}C NMR and DEPT spectra are shown in Figures SM 4.1.3.5.2 - SM 4.1.3.5.7 and SM 4.1.3.5.9 - SM 4.1.3.5.12.

All NMR spectra are in accordance with the proposed structures and with the spectra reported for similar compounds in the mentioned literature. 1H NMR spectrum of the squarylium cyanine dye **6** shows a typical peak as a singlet of two hydrogens at 5.807 ppm corresponding to the methynic chain. The reproducibility of this experiment was assessed by its repetitive execution (sixfold) by six students of the 1st year of the Biochemistry M.Sc. from University of Trás-os-Montes e Alto Douro.

Table SM 4.1.3.5.1 – Yield, m.p. and IR spectra of **3**, **4** and **6** compounds.

Compound	6-iodoquinaldine (3)	quaternary salt 4	squarylium cyanine dye 6
Yield (%)	38-45*	50-90	40-50
m.p. (°C)	110-111	219-221	>300
IR (KBr, ν_{\max} , cm^{-1})	1604, 1590, 1479, 1376, 1292, 1119, 881, 825, 807	3050, 2936, 1597, 1504, 1461, 1373, 1164, 885, 726	2924, 1616, 1583, 1545, 1474, 1444, 1350, 1309, 1255.

*Taking into account only the crystals obtained in the first recrystallization

Photo of the experiment

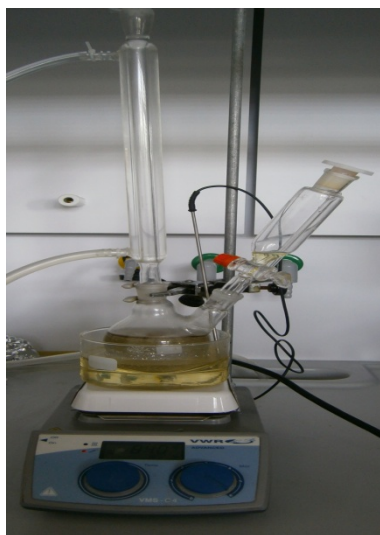


Figure SM 4.1.3.5.1 Fitting for synthesis of 6-iodoquinaldine (**3**).

^1H , ^{13}C and DEPT NMR spectra

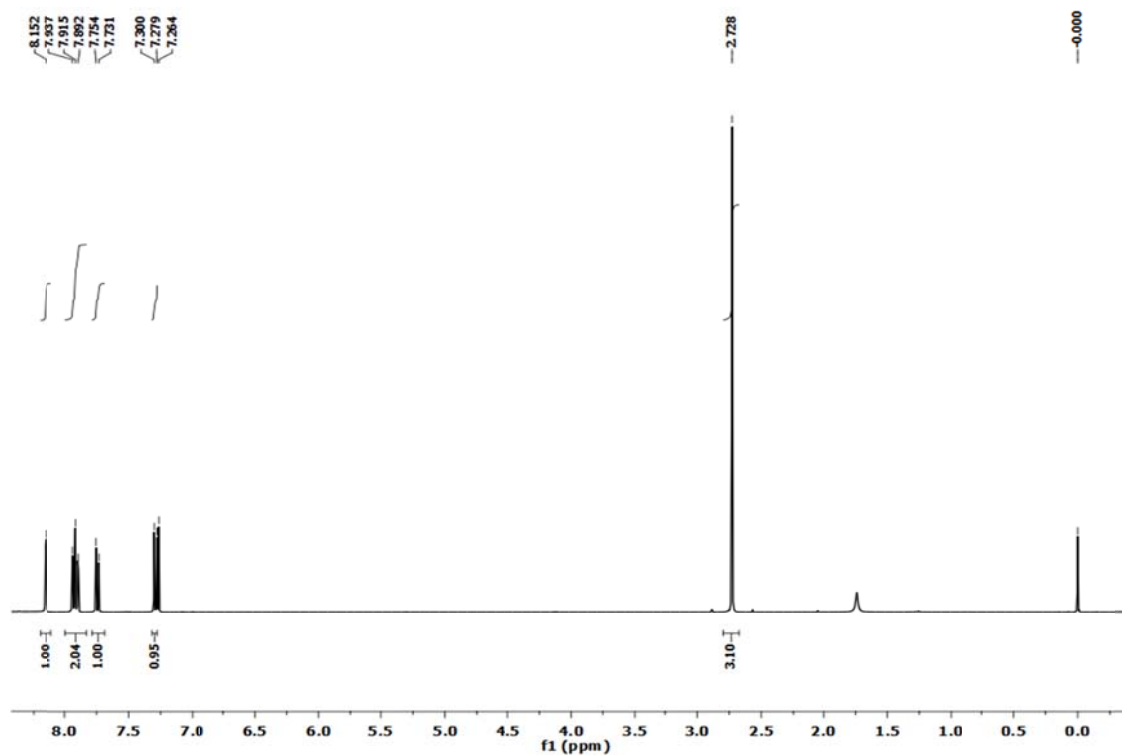


Figure SM 4.1.3.5.2 – ^1H NMR spectrum (400 MHz, CDCl_3) of 6-iodoquinaldine (3).

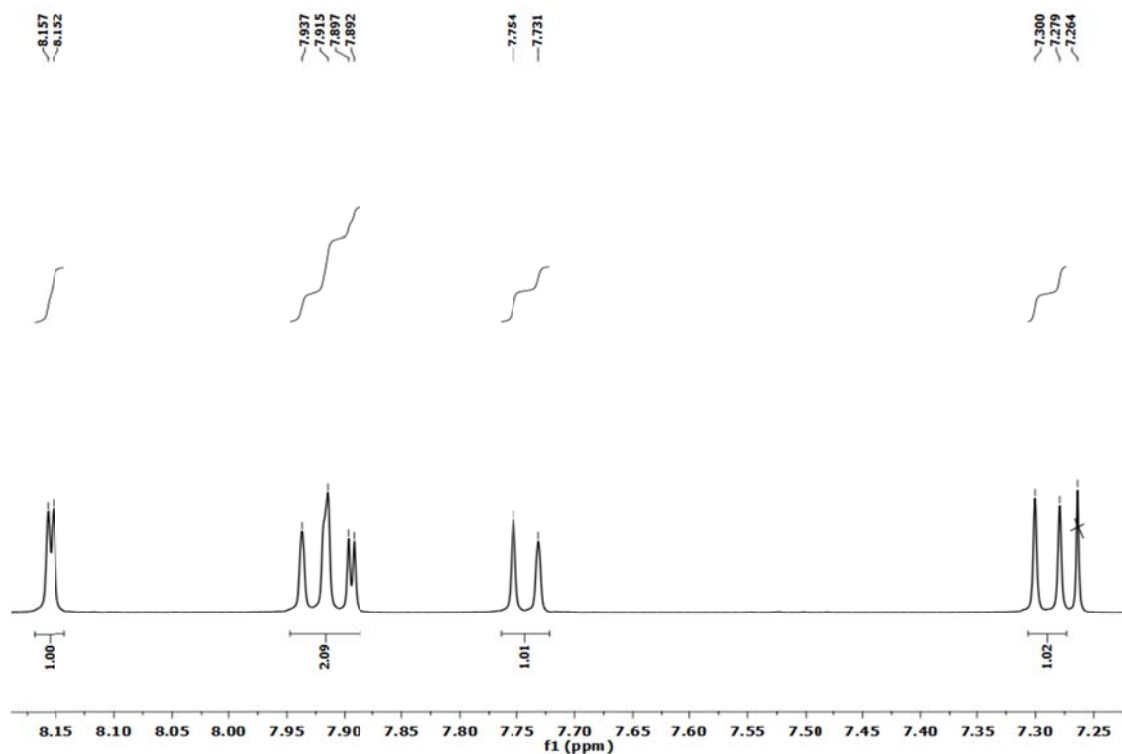


Figure SM 4.1.3.5.3 – ^1H NMR spectrum detail showing the aromatic peaks of 6-iodoquinaldine (3).

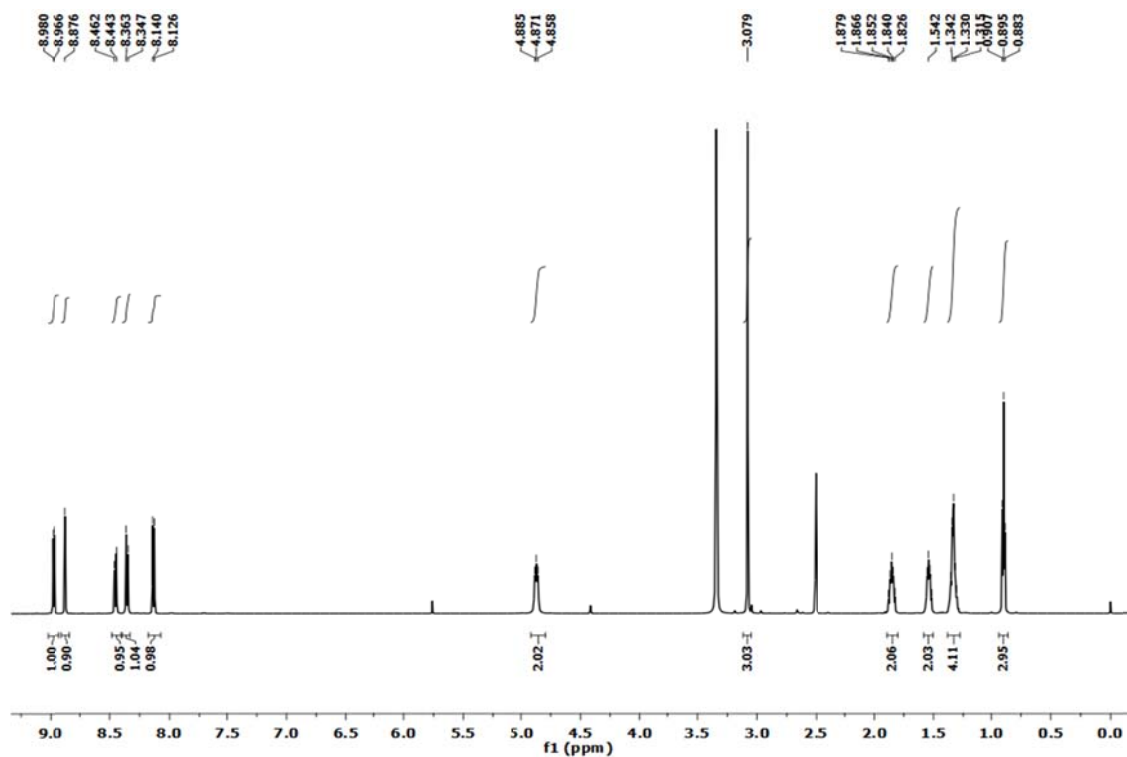


Figure SM 4.1.3.5.4 – ^1H NMR spectrum (600 MHz, DMSO-d_6) of quaternary salt 4.

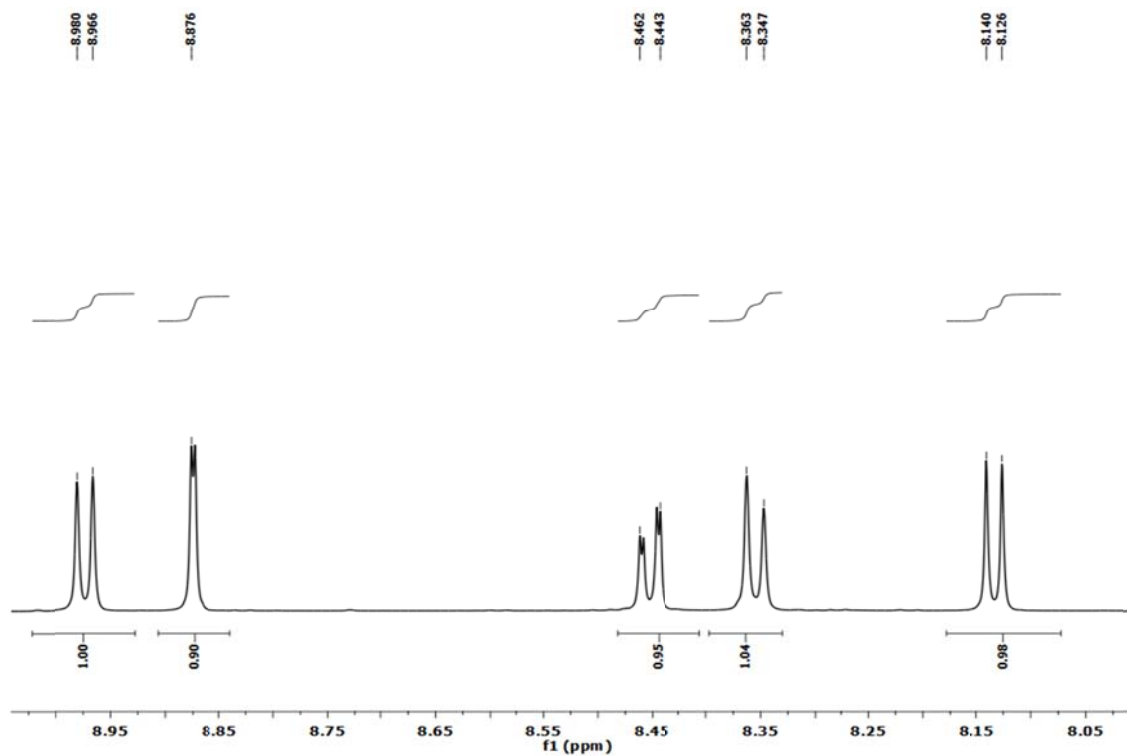


Figure SM 4.1.3.5.5 – ^1H NMR spectrum detail showing the aromatic peaks of quaternary salt 4.

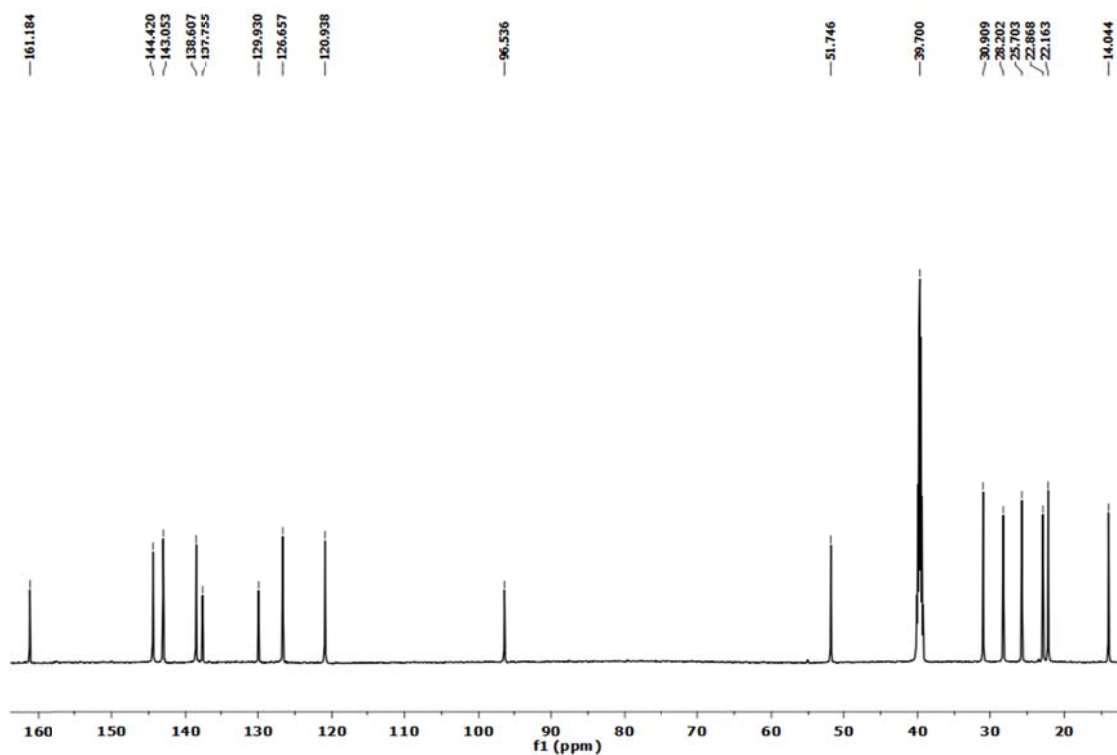


Figure SM 4.1.3.5.6 – ¹³C NMR spectrum (600 MHz, DMSO-d₆) of quaternary salt 4.

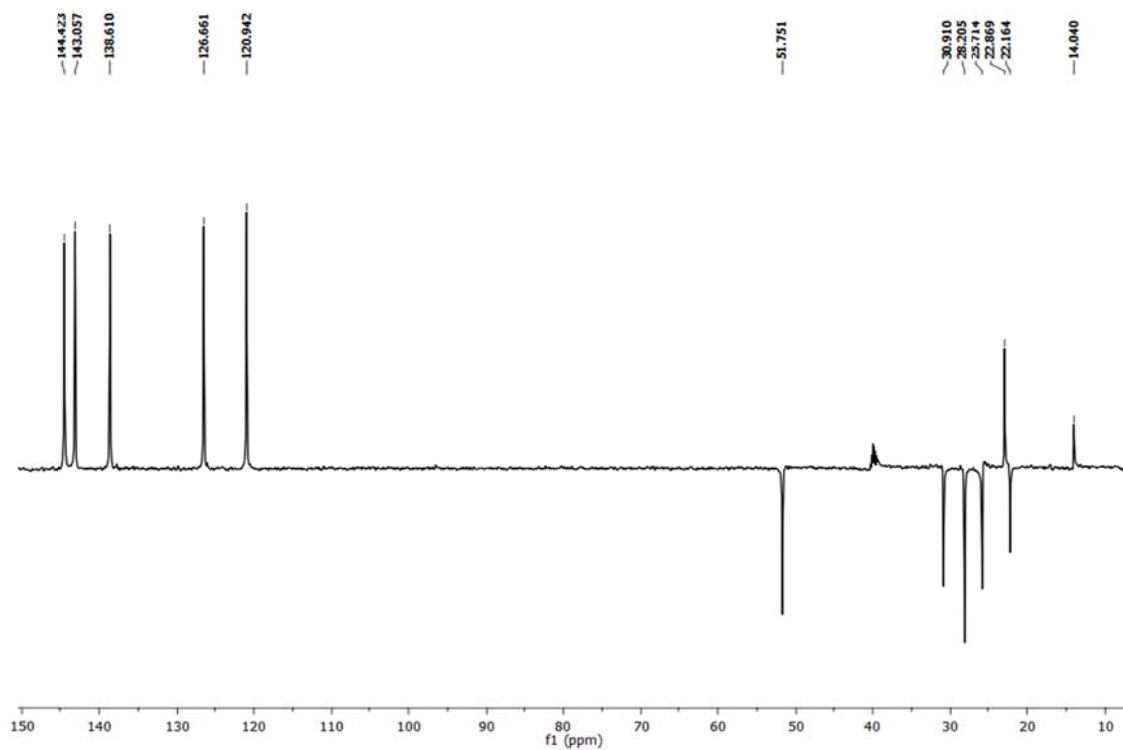


Figure SM 4.1.3.5.7 – DEPT 135 spectrum (600 MHz, DMSO-d₆) of quaternary salt 4.

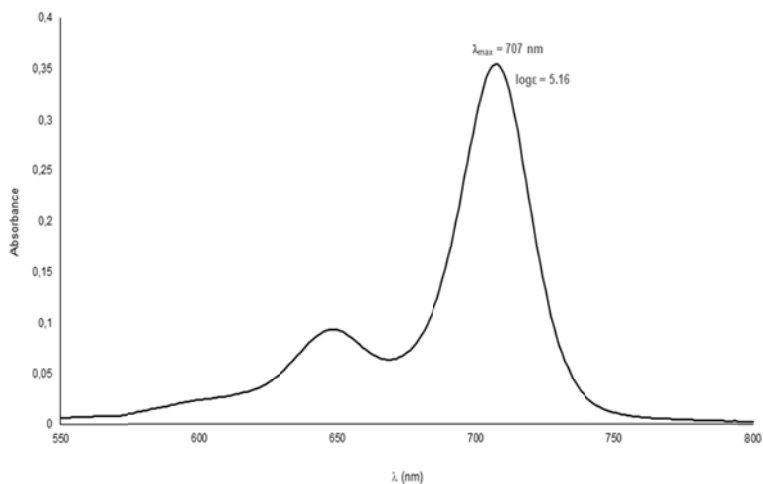


Figure SM 4.1.3.5.8 –Visible spectrum (CH_2Cl_2) of squarylium cyanine dye 6.

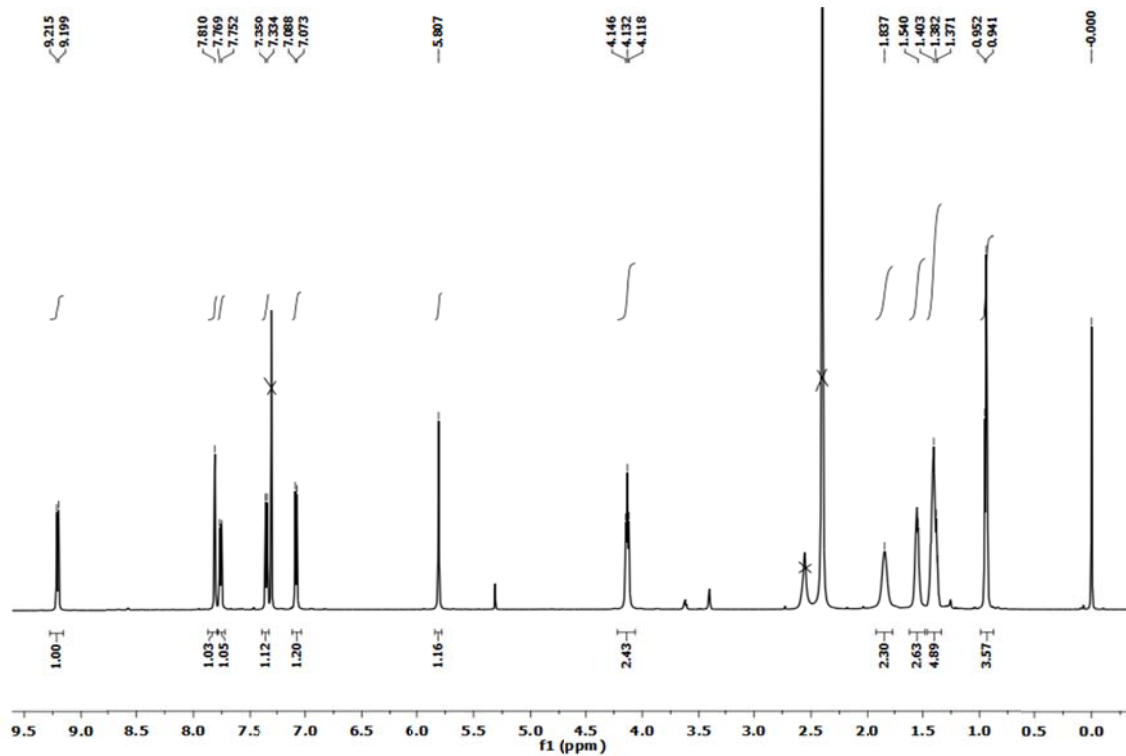


Figure SM 4.1.3.5.9 – ^1H NMR spectrum (600 MHz, $\text{CDCl}_3 + \text{MeOD}$) of squarylium cyanine dye 6.

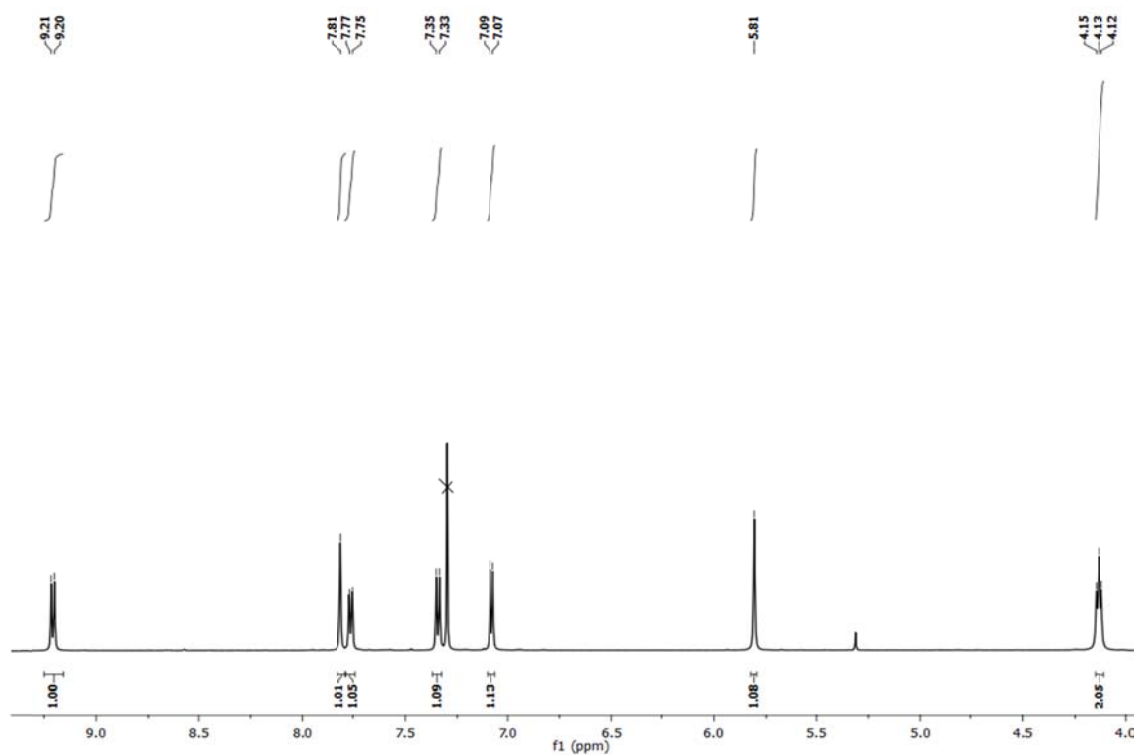


Figure SM 4.1.3.5.10– ^1H NMR spectrum detail showing the aromatic peaks of squarylium cyanine dye 6.

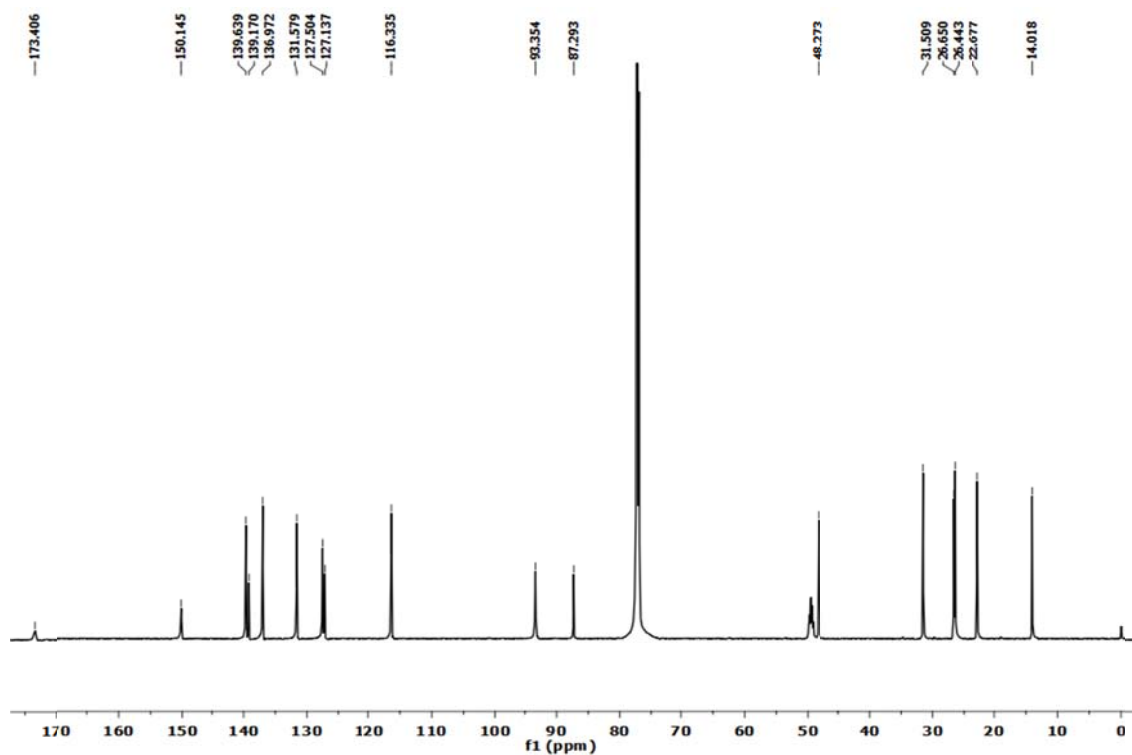


Figure SM 4.1.3.5.11 – ^{13}C NMR spectrum (600 MHz, $\text{CDCl}_3 + \text{MeOD}$) of squarylium cyanine dye 6

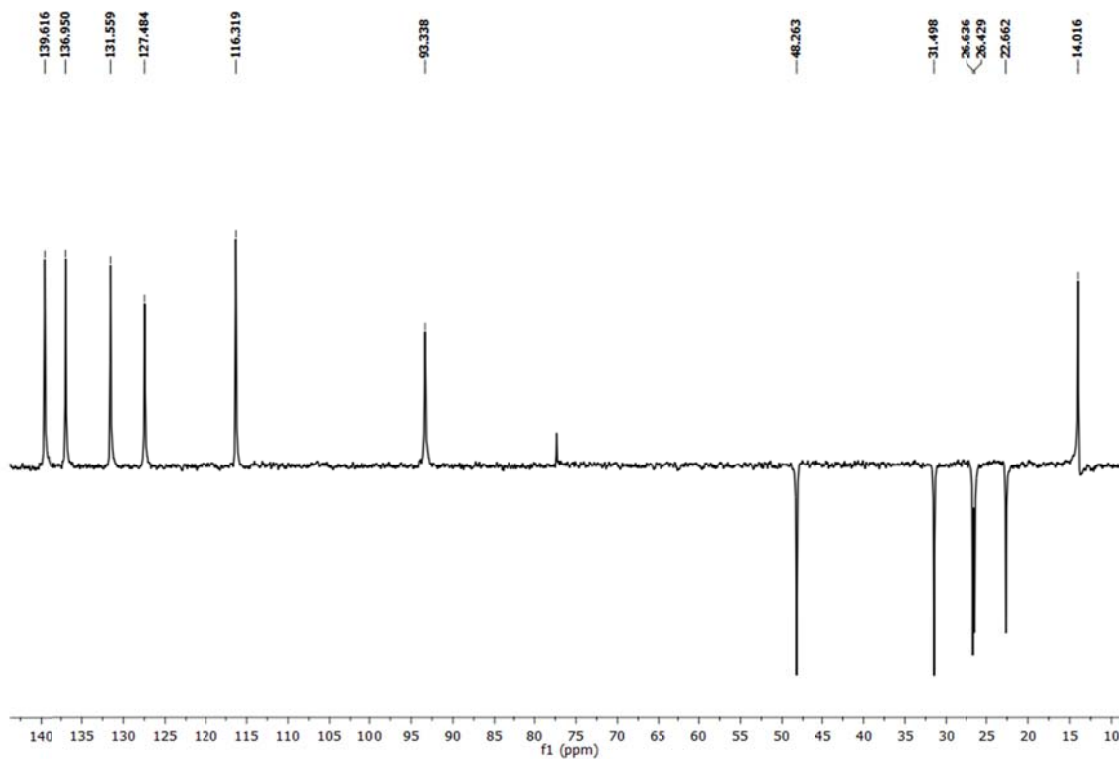


Figure SM 4.1.3.5.12 – DEPT 135 spectrum (600 MHz, DMSO-d₆) of squarylium cyanine dye **6**.